Distribution Agreement

In presenting this thesis as a partial fulfillment of the requirements for a degree from Emory University, I hereby grant to Emory University and its agents the non-exclusive license to archive, make accessible, and display my thesis in whole or in part in all forms of media, now or hereafter now, including display on the World Wide Web. I understand that I may select some access restrictions as part of the online submission of this thesis. I retain all ownership rights to the copyright of the thesis. I also retain the right to use in future works (such as articles or books) all or part of this thesis.

Hithardhi Duggireddy April 14, 2020

Pre-Ictal Window Identification via Logistic Regression

By

Hithardhi Duggireddy

Robert Gross M.D. Ph.D.
Advisor

Neuroscience and Behavioral Biology

Robert Gross M.D. Ph.D.
Advisor

Michael Crutcher Ph.D.
Committee Member

Annaelle Devergnas Ph.D.
Committee Member

Mark Connolly B.S.
Committee Member

2020

Pre-Ictal Window Identification via Logistic Regression

By

Hithardhi Duggireddy

Robert Gross M.D. Ph.D.
Advisor

An abstract of
a thesis submitted to the Faculty of Emory College of Arts and Sciences
of Emory University in partial fulfillment
of the requirements of the degree of
Bachelor of Science with Honors

Neuroscience and Behavioral Biology

2020

Abstract

Pre-Ictal Window Identification via Logistic Regression

By Hithardhi Duggireddy

Epilepsy is a debilitating disease characterized by spontaneous recurring seizures. It is the 4th most common neurological disorder. Mesial temporal lobe epilepsy (MTLE) is the most prevalent form of epilepsy and is the most resistant to medical therapy, with over 30% of patients failing to achieve adequate seizure control with antiepileptics. These patients may require surgery, but, resection of the epileptic focus is often not possible. An alternative therapy for these patients may be neural modulation via electrical stimulation; however, patients currently only experience approximately a 50% reduction in seizure frequency. A better fundamental understanding of mechanisms underlying seizure transition may be necessary for neural modulation to become more effective as a prophylactic therapeutic. Currently, research is being done to develop seizure prediction models to aid neural modulation; however, the pre-ictal windows used to develop these models are chosen arbitrarily. Therefore, the objective of this study was to develop a method to quantitatively delineate the pre-ictal window in order to prevent arbitrary pre-ictal window selection in seizure prediction models in order to improve neural modulation techniques and improve the understanding of neural dynamics that underlie seizure transition. By using a sliding window logistic regression classifier, we were able to test a spectrum of ground truths for a hypothesized pre-ictal window in a tetanus toxin (TeNT) rat model of epilepsy and in a non-human primate (NHP) penicillin (PCN) model of epilepsy. Results revealed that our classifier was able to distinguish between pre-ictal and interictal windows, which were validated by AUC values greater than 0.5 and the presence of AUC plateaus, which were characterized by consecutive pre-ictal window durations with similar receiver operating characteristics (ROC) curves and AUC values. Our tool has made it possible to quantitatively delineate the pre-ictal window on a subject-specific basis and compare the pre-ictal neural dynamics between different seizure models.

Pre-Ictal Window Identification via Logistic Regression

By

Hithardhi Duggireddy

Robert Gross M.D. Ph.D.
Advisor

A thesis submitted to the Faculty of Emory College of Arts and Sciences
of Emory University in partial fulfillment
of the requirements of the degree of
Bachelor of Science with Honors

Neuroscience and Behavioral Biology

2020

Acknowledgements

I would like to thank Mark Connolly for giving me the privilege to begin my research career 3 years ago as his mentee and for his incredible help, guidance, and support throughout my time at Emory. I would like to thank Dr. Robert Gross and Dr. Annaelle Devergnas for allowing me to conduct research in their labs, providing me with guidance, and along with Dr. Michael Crutcher for taking the time to support me in my research and academic career. I would also like to thank Dr. Lena Ting and Mr. Luke Drnach for helping me solidify the fundamental skills needed to succeed in the world of computational neuroscience during my Beckman Scholars fellowship. I would also like to thank Dr. Sharanya Desai and Dr. Sang Park for generating the Rat-TeNT data used in this research and Dr. Annaelle Devergnas for generating the NHP-PCN data used in this research.

Table of Contents:

Abstract

Epilepsy is a debilitating disease characterized by spontaneous recurring seizures. It is the 4th most common neurological disorder. Mesial temporal lobe epilepsy (MTLE) is the most prevalent form of epilepsy and is the most resistant to medical therapy, with over 30% of patients failing to achieve adequate seizure control with antiepileptics. These patients may require surgery, but, resection of the epileptic focus is often not possible. An alternative therapy for these patients may be neural modulation via electrical stimulation; however, patients currently only experience approximately a 50% reduction in seizure frequency. A better fundamental understanding of mechanisms underlying seizure transition may be necessary for neural modulation to become more effective as a prophylactic therapeutic. Currently, research is being done to develop seizure prediction models to aid neural modulation; however, the pre-ictal windows used to develop these models are chosen arbitrarily. Therefore, the objective of this study was to develop a method to quantitatively delineate the pre-ictal window in order to prevent arbitrary pre-ictal window selection in seizure prediction models in order to improve neural modulation techniques and improve the understanding of neural dynamics that underlie seizure transition. By using a sliding window logistic regression classifier, we were able to test a spectrum of ground truths for a hypothesized pre-ictal window in a tetanus toxin (TeNT) rat model of epilepsy and in a non-human primate (NHP) penicillin (PCN) model of epilepsy. Results revealed that our classifier was able to distinguish between pre-ictal and interictal windows, which were validated by AUC values greater than 0.5 and the presence of AUC plateaus, which were characterized by consecutive pre-ictal window durations with similar receiver operating characteristics (ROC) curves and AUC values. Our tool has made it possible to quantitatively delineate the pre-ictal window on a subject-specific basis and compare the pre-ictal neural dynamics between different seizure models.

I. INTRODUCTION

Epilepsy is a debilitating disease characterized by spontaneous recurring seizures. It is the fourth most common neurological disorder with 65 million people afflicted globally (England *et al*., 2012). Those afflicted experience significant burden due to disability caused by the disease. The pathophysiology and etiology of epilepsy is still relatively unknown, which makes determining appropriate treatment plans for the condition difficult (Stafstrom & Carmant, 2015). At present, we know that a seizure occurs due to a hypersynchronous discharge of neurons in the brain, which is speculated to have a multitude of causes across many levels of neural functioning from genetic and cellular abnormalities to mass neuronal circuit dysfunctions (Stafstrom & Carmant, 2015).

The ambiguity in the etiology of epilepsy and the heterogeneity of seizures, make this a challenging disease to treat, with over one-third of patients failing to achieve adequate seizure control with antiepileptics (Perucca, 2014). In addition, these patients are also very prone to adverse effects, with prevalence peaking at 40%, which causes up to 30% of patients to discontinue antiepileptic medication (Perucca, 2014). Uncontrolled or poorly managed epilepsy takes a major toll of quality of life, as it increases risk of sudden accidental death, reduces employment opportunities, hinders psychosocial functioning, and impairs cognition (Willems, *et al*., 2018).

Mesial temporal lobe epilepsy (MTLE), the focus of our study, is the most prevalent form of epilepsy and unfortunately, also happens to be the most resistant to medical therapy (Min *et al*. 2013). MTLE involves the internal structure of the temporal lobe, with the epileptic focus often located in the hippocampus or its surrounding area. Typically, 80% of temporal lobe epilepsy cases are classified as MTLE (Blair, 2012). MTLE etiology, like most forms of epilepsy, is relatively unknown. Often times, a traumatic brain injury (TBI) during youth, prolonged febrile seizures, or

general head trauma are triggers (Blair, 2012). In addition to seizures, those with MTLE suffer from additional memory and mood deficits, which also don't resolve with administration of antiepileptics (Blair, 2012).

Therefore, over 30% of patients with intractable MTLE require surgery, most often in the form of an anterior temporal lobectomy (ATL) (Barr, 2016). This procedure involves the resection of the inferior and middle temporal gyri, uncus, part of the amygdala, and approximately 2-3 cm of the hippocampus and parahippocampal gyrus (Al-Otaibi, 2012). ATL provides the benefit of potential seizure freedom and a significant reduction in daily medication post-operation (Barr, 2016). Although ATL has its benefits, not all patients with intractable MTLE can opt for the procedure. There are patients where resection of the anterior temporal lobe may not be feasible due to the location of the seizure focus and there are other patients that would face greater risks in the form of language and memory deficits than benefits from the resection (Martin *et al.*, 2002). Furthermore, despite the claimed benefits, patients may not want areas of their brain totally resected, as this procedure cannot be reversed. Patients with intractable MTLE that don't respond to medication and aren't candidates for/don't want to opt for surgical resection need another treatment option.

An alternative therapy for these patients may be neural modulation via electrical stimulation, such as deep brain stimulation (DBS) or responsive neurostimulation (RNS). The principle of electrical neural modulation is to regulate endogenous processes via exogenous electrical stimulation through the implantation of electrodes in the target brain region (Nune *et al.*,2015). Generally, in the case of epilepsy, recording and stimulating electrodes are implanted at the localized epileptic focus, a region of epileptic spread, or a region that projects to the epileptic focus (Schulze-Bonhage, 2016). The recording electrode(s) monitor neural activity via

electrocorticographic recordings and stimulating electrodes can be either programmed to deliver constant electrical pulses (open-loop) or only stimulate during the detection of abnormal activity (closed-loop) that may be classified as seizure (ictal) activity (Ghasemi *et al.* 2018). The closed-loop neural modulatory device reacts by delivering electrical stimulation via the stimulating electrode(s) in order to disrupt the epileptic signal and return neural activity to baseline. This closed-loop model of neural modulation is employed by the RNS (Sun & Morrell, 2014). DBS utilizes an open-loop model of neural modulation, meaning that it delivers a fixed pattern of electrical stimulation that is not driven by seizure detection; rather, its goal is to maintain baseline neural activity through constant modulation (Ghasemi *et al*. 2018).

Despite the growing success of neural modulation, patients only experience approximately a 50% reduction in seizure frequency with few becoming seizure free (Laxpati *et al.*, 2014). There are also additional disadvantages in the techniques employed by RNS and DBS. For RNS, the most significant disadvantage is that it's a reactive therapy, rather than a proactive therapy. By the time a seizure is detected, and the RNS reacts to it, it may be too late to abort the seizure (Sun & Morrell, 2014). DBS on the other hand, may provide more stimulation than necessary, as it is constantly active, which has been linked to potential memory impairments, is cost-ineffective (battery issues), and its mechanism of action is poorly understood (Zangiabadi *et al*., 2019). The disadvantages of both of these techniques stem from knowledge gaps in the neural dynamics of seizures and underlying epileptiform neural states. Specifically, ambiguity in what characterizes the transition between different epileptiform neural states are a limiting factor to furthering the success rate of neural modulation (Carney, 2011).

Without the fundamental understanding of the mechanisms underlying the transition from the asymptomatic brain to that experiencing a seizure, neural modulation techniques may struggle

to become more effective as seizure prevention measures. One potential method to improve neural modulation therapies for the treatment of epilepsy would be through the study of the transition from an interictal to pre-ictal period (Carney, 2011). Characterizing the neural activity prior to a seizure will lead to the development of better seizure prediction models, which is an important next step for the advancement of neural modulation (Iasemidis, 2011). Since a key component in seizure prediction is being able to accurately delineate the transition from the non-seizure (interictal) state to the ictal state, it is vital that this transition period preceding ictal activity, known as the pre-ictal window, be closely studied to better understand the dynamics of seizure onset (Cook *et al*. 2013). The delineation of a pre-ictal window will allow researchers to better predict seizures in order to improve techniques for the tuning of stimulation parameters in prophylactic neural modulation therapies for epilepsy (Nagaraj *et al*., 2015). Although, research has already been done on seizure-prediction models, current seizure prediction methods use arbitrarily selected pre-ictal windows (DiLorenzo *et al.*, 2019) (Kiral-Kornek *et al*., 2018) (Alotaiby *et al*., 2017). The subjective nature of this approach leads to lack of consistency across seizure prediction models, the inclusion of superfluous data, biased results, and minimal progress in the understanding of neural dynamics characterizing the transition to seizure.

The objective of this study was to develop a method to quantitatively delineate the pre-ictal window on a subject-specific basis and to compare pre-ictal neural dynamics between different seizure models using a supervised machine learning classification model. From this study, electrophysiological neural features that characterize the pre-ictal window can be identified and studied to better understand the transition from the interictal state to the ictal state and also used to identify the appropriate, subject-specific stimulation patterns for modulating neural state.

II. METHODS

A. Data Collection: NHP-PCN

Local field potential (LFP) data was recorded from a non-human primate (NHP, rhesus macaque) penicillin (PCN) model of seizures. LFP is the measure of the electric potential, the summation of excitatory and inhibitory dendritic potentials, recorded in the extracellular space in neural tissue. The NHP-PCN model is characterized by spontaneous, frequent, and reproducible seizures that can be induced in a controlled manner via intrahippocampal injection of penicillin (Sherdil *et al.,* 2018). Furthermore, the NHP-PCN model of epilepsy presents with hippocampal sclerosis, a common feature of MTLE in the clinical setting, and has similar symptomatogenic and irritative zones to humans with MTLE. (Sherdil *et al.,* 2018). Therefore, results from analysis of the NHP-PCN model has the potential to provide good clinical translational value.

In order to obtain LFP recordings from the NHP, surgery was performed to implant a chamber for acute recording and stimulation, electrocorticography (ECOG), and a head-fixation system (Crist Instrument Company, Hagerstown, MD) (Sherdil *et al*., 2018). The NHP was head-fixed to an NHP behavioral chair while a motorized microdrive (NAN Instruments, Israel) was attached to the implanted chamber. After a brief recovery period, mapping was performed next to determine the proper hippocampal coordinates for the electrodes. The implanted chamber covers a large area and has a fine grid of holes on top demarcated with coordinates. We estimated the location of the hippocampus based on pre- and post-operative MRIs and based on an anatomical atlas (Martin and Bowden). From the chamber's grid, we chose E5 as the coordinate that we would next drive two 12-contact electrodes (Heraeus, St. Paul, MN) through into the hippocampal region. To ensure that the electrodes were in the proper location, we monitored

single-unit (SU) recordings. After 5-10 minutes of rest to account for acute deformities in the brain, approximately 12,000 IU of PCN was injected at a rate of 1 µL//min via a cannula in the midpoint of the implanted electrodes. The tubing from the injection system was then clamped with a hemostat in order to prevent leakage of PCN to neural structures dorsal to the hippocampus as the cannula was withdrawn (Sherdil *et al*., 2018).

After injection of PCN, interictal spikes in the hippocampus appeared within 5 minutes, with the first seizure occurring within 10 minutes post-injection. Shortly after, we would observe the manifestation of electrographic seizures and begin recordings. LFP were recorded through a BlackRock Cerebus data acquisition system. The sampling rate of our recordings was 2000 Hz. Spontaneous, transient seizures would occur for approximately 3-5 hours post-PCN injection. Recordings were obtained until the last seizure occurrence exceeded 30 minutes (*Sherdil* et al., 2018).

B. Data Collection: Rat-TeNT

Local field potential (LFP) data was recorded from a rat (Sprague Dawley rat) tetanus toxin (TeNT) model of seizure. The rat-TeNT model is characterized by a window (3-5 days) of frequent, spontaneous, heterogenous seizures, which provides a large amount of data in a short amount of time (Desai *et al.*, 2016). Since this is a non-lesional model of MTLE, we have more confidence in the location of the epileptic focus, as brain lesions can cause the spread of seizures. This is, therefore, an excellent model to study non-sclerosing MTLE.

In order to obtain LFP recordings from the rats, surgery was performed to implant a 16-channel TDT array (Tucker-Davis Technologies) (N = 11 rats) in a rat's hippocampus (Desai *et al.*, 2016) (Park *et al*., 2019). A craniectomy was performed over the right dorsal hippocampus and the cerebellum. Using a Nanoject microinjection device, 45 ng of tetanus toxin in 0.5

microliters of sterile phosphate-buffered saline (PBS) was injected into the right dorsal hippocampus. 5 of the rats were also injected with AAV5-hSynapsinhChR2(H134R)-EYFP for another unrelated optogenetic experiment (Park *et al*., 2019). One skull screw was attached over the cerebellum to serve as the reference for recorded data and four other skull screws served as ground for stimulation purposes. The craniectomies were closed with the application of dental acrylic. The rats had a 1-week post-surgery recovery period.

Spontaneous Racine scale 5 Seizures were induced in TeNT rats 5 to 7 days post-surgery. During this period, LFP activity in the rats was recorded using either NeuroRighter, which is an open-source system for multi-channel electrode closed-loop recording and/or stimulation (Desai *et al.*, 2016), or using TDT, which is another open source system used for multi-channel electrode recording and/or stimulation (Park *et al*., 2019). A recording headstage was attached to the rats, which were placed in Plexiglass chambers, and a commutator was used to allow for rats to move freely during recording sessions. The sampling rate of all recordings was 2000 Hz. Seizure frequency peaked and was most consistent for 3-5 consecutive days 1-week post-surgery.

C. Data Processing

The data from the both models of epilepsy were annotated with seizure onset and offset times. Rat-TeNT data was annotated during the recording session itself. A seizure was only counted if it was either a Racine scale 4 (rearing) or Racine scale 5 (rearing and falling). Following recording sessions, rat-TeNT data was also annotated for electrographic seizures by at least 2 observers, whose times were reconciled at the end (Desai *et al.*, 2016). NHP-PCN data was annotated following the recording sessions by at least 2 observers. Video recordings were simultaneously presented in “real-time” with EEG recordings of the LFP. Seizure onset and offset times were recorded by the observers and reconciled at a later date.

The LFP data, both rat-TeNT and NHP-PCN, was also filtered to remove potential artifacts. First, the data was run through a notch filter set in the range of 58 Hz to 62 Hz. This was done to remove 60 Hz noise caused by electrical output. Next a highpass filter was implemented at 2 Hz in order to remove oscillatory motion from cables hooked to the animals' heads. Lastly, the data was also run through a lowpass filter set to 150 Hz in order to disregard all frequencies above 150 Hz. All filtering incorporated zero-phase digital filtering and a Butterworth filter design.

Using the seizure annotations, the filtered LFP data was labeled with seizure start and stop times. The LFP data was then segmented to obtain the interictal period between two seizures. The new LFP segments only contain one seizure and its preceding interictal period until the end of the previous seizure (i.e. an interictal period plus an ictal period) (Fig. 1).

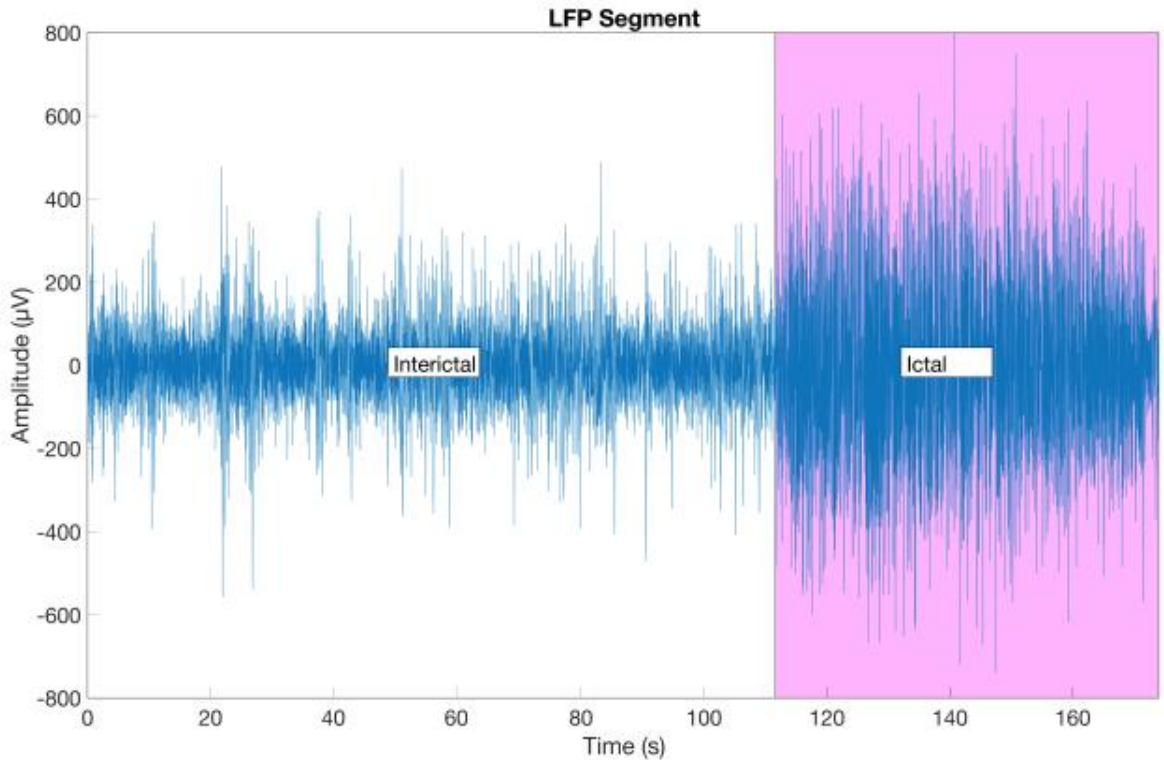

Fig. 1: *Annotated and segmented LFP from NHP-PCN used for subsequent feature extraction showing distinction between interictal and ictal periods.*

D. Feature Extraction

In order for our classifier to identify our hypothesized pre-ictal state from the interictal ("baseline") state, we decided to train it using frequency domain features. In order to extract frequency domain features from our LFP data, the mean power of the 5 canonical frequency bands (i.e. alpha, beta, gamma, delta, theta) were estimated using the Multi-Taper Method (MTM) for each LFP segment (Bababi & Brown, 2014).

The MTM is an adaptation of the Fourier transform. This method was chosen to extract spectral features, as it is generally considered to provide one of the most accurate frequency domain estimates. The MTM calculated our desired spectral features by initially windowing interictal period data into 0.5-second overlapping windows (0.01 second overlap) and computing a Fourier transform for each of the windows. This results in independent estimates of the power spectral density (PSD) of each window or "taper". The orthogonal tapers are then averaged to give a better estimate of the frequency domain since the resulting frequency domain estimate will have a lower variance than if only one Fourier transform was taken for the entire interictal period at once (Bababi & Brown, 2014).

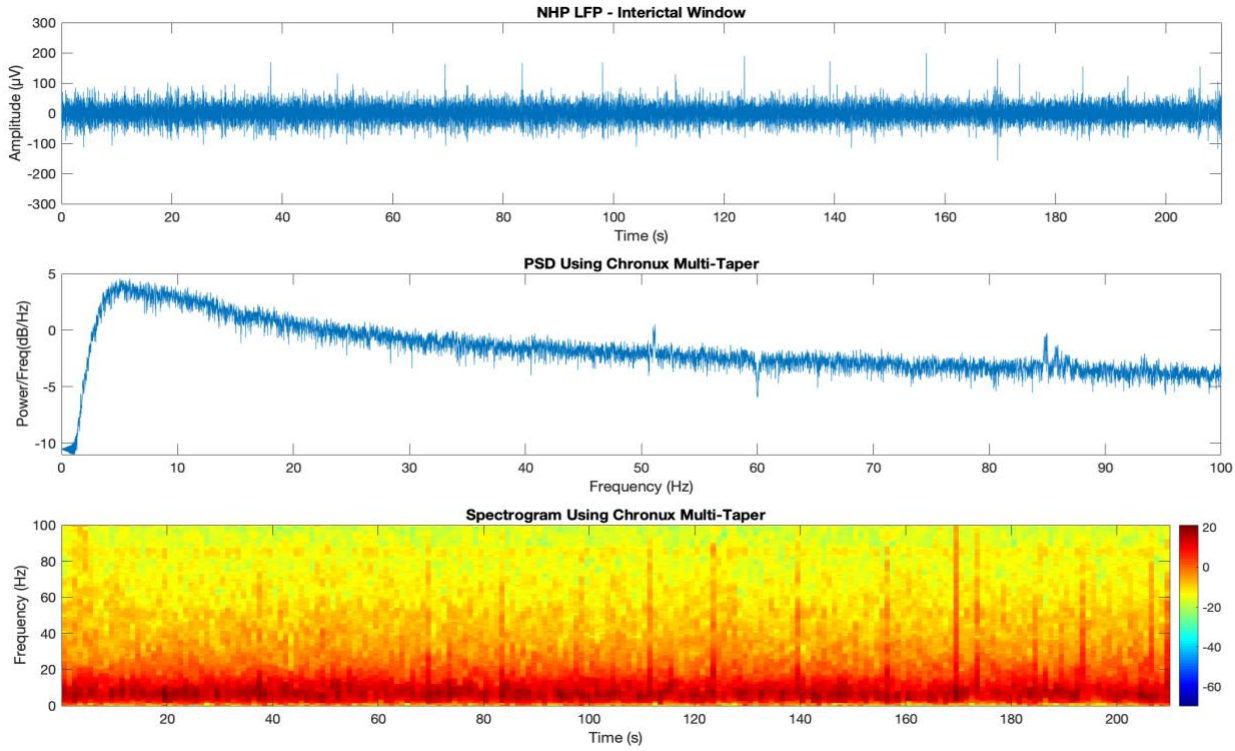

Fig. 2a: *Example of NHP-PCN interictal window presented in time domain, as a power spectral density, and as a spectrogram calculated using MTM. Depicts conversion from time to frequency domain in order to extract spectral features.*

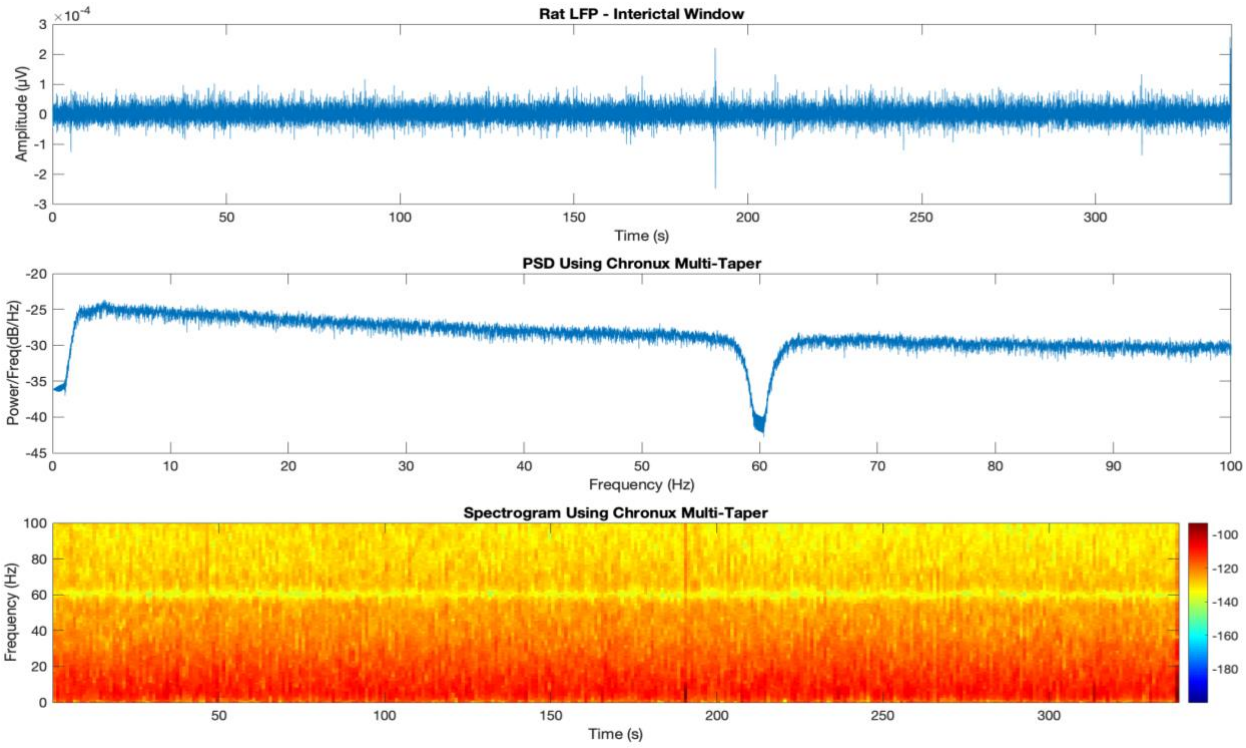

Fig. 2b: *Example of Rat-TeNT interictal window presented in time domain, as a power spectral density, and as a spectrogram calculated using MTM. Depicts conversion from time to frequency domain in order to extract spectral features.*

Since our study's focus is on the dynamics that precede a seizure (i.e. pre-ictal window), only the interictal period's frequency features were estimated using MTM (Fig. 2a and 2b). The following criteria was established in the extraction of these frequency bands: delta [0-4 Hz], theta [4-8 Hz], alpha [8-13 Hz], beta [13-32 Hz], Gamma [32-60 Hz] (Myers *et al. 2017)*. We referred to the mean power of these 5 spectral frequency bands as electrophysiological neural features (ENFs).

E. Supervised Learning: Logistic Regression

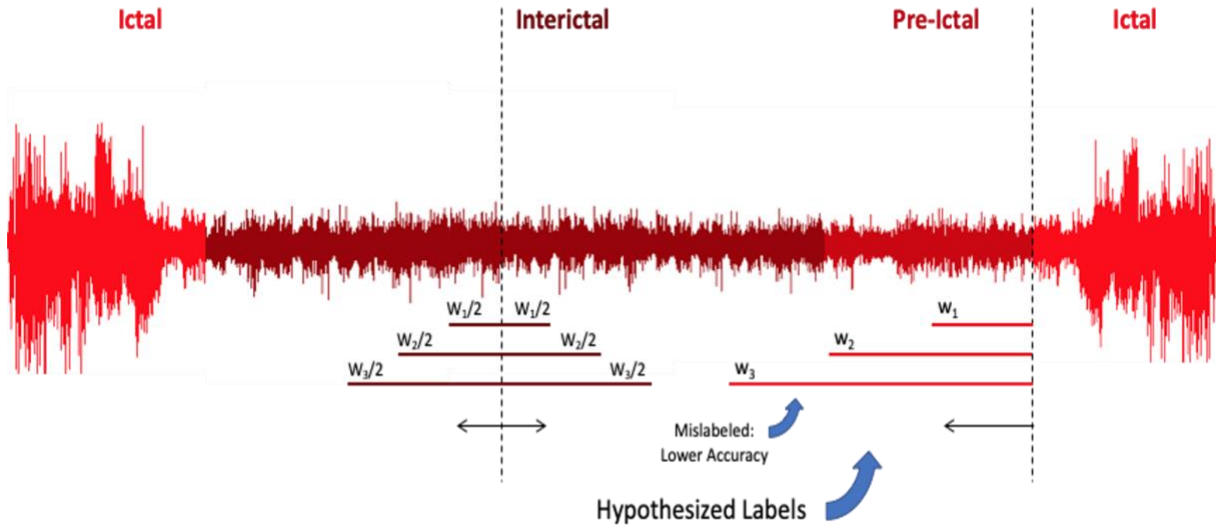

Fig. 3: *Diagram of logistic regression classifier with sliding window.*

In order to identify the pre-ictal window, we utilized a supervised learning algorithm – logistic regression. Logistic regression is a classification algorithm used when there is a categorical response variable. In this case, our response variable was "pre-ictal", represented by a "1", or "interictal", represented by a "0". Logistic regression aims to find a relationship between features that may represent one of the categorical outcomes and the probability of a specific outcome. In the context of this study, logistic regression is trained to estimate the probability that data

consisting of ENFs from a specific time window is either pre-ictal or interictal (baseline) (Bewick *et al.*, 2005).

We asserted a spectrum of hypothesized ground truth corresponding to the duration of the pre-ictal window by utilizing a sliding window (Fig. 3). We established the interictal window *a priori*, but tested various durations of the pre-ictal window, as this window length is not known. The duration of the interictal window was balanced with the duration of the hypothesized pre-ictal window (i.e. If the pre-ictal window being tested was 10 seconds long, that data was compared with a 10-second-long interictal window). We used the time directly in the middle of two consecutive seizures to serve as the starting point for the interictal windows and the time of seizure onset to serve as the starting point for all hypothesized pre-seizure windows. A constant amount of data was subsampled for each window length, which was then fed into the logistic regression classifier. This was done as classifier performance is likely to increase as more data is given and could be a potential confounding variable when determining pre-ictal window duration. A K-fold cross-validation was performed (K = 5) on the data in order to assess the generalizability of our classifier by ensuring that our classifier wasn't simply "memorizing" data and overfitting in order to increase performance (Little *et al*., 2017).

The receiver operating characteristics (ROC) curve was calculated for each pre-ictal window length and its corresponding area under the curve (AUC) was calculated (Bewick *et al.*, 2005). We used the AUC as our metric to discern whether or not a pre-ictal window could be discriminated from the interictal window it was being compared to of equal duration. The goal of our classification model was to use a sliding window to test the hypothesis that data from a pre-ictal window of a given length may be discriminated from an equal length interictal window.

F. Classification: NHP-PCN

We used data from 10 total NHP-PCN recordings of the same NHP to train our classifier. After removal of data containing high levels of artifact, the total remaining number of seizures were n = 24. Pre-ictal window identification was performed by training the classifier with a subset of these seizures and testing on a new subset of seizures from the same animal. The resulting pre-ictal window classification represented data across different days of recording for the same NHP. Training and testing were done in this manner to see if the classifier could generalize between different days' recording sessions, as seizures induced via PCN may be heterogenous when compared between multiple recordings/days.

G. Classification: Rodent TeNT

We used data from 11 different rats (n = 200 seizures) to train and test our classifier in a joint analysis of all rats. This was done to see if the classifier could generalize between seizures of different days and varying presentations between animals. Since TeNT-induced seizures are very heterogenous, proper pre-ictal window classification would necessitate that the classifier be able to generalize between various presentations of seizure. Pre-ictal window identification was also performed on individual animal's that had at least 20 artifact-free seizure recordings available. This resulted in an individual analysis of 3 rats. This was done to have a comparison to the individual NHP analysis and to see how classifier performance differs between a joint analysis of several different animals across multiple recording days and an analysis of the same animal across multiple recording days.

III. Results

A. NHP-PCN

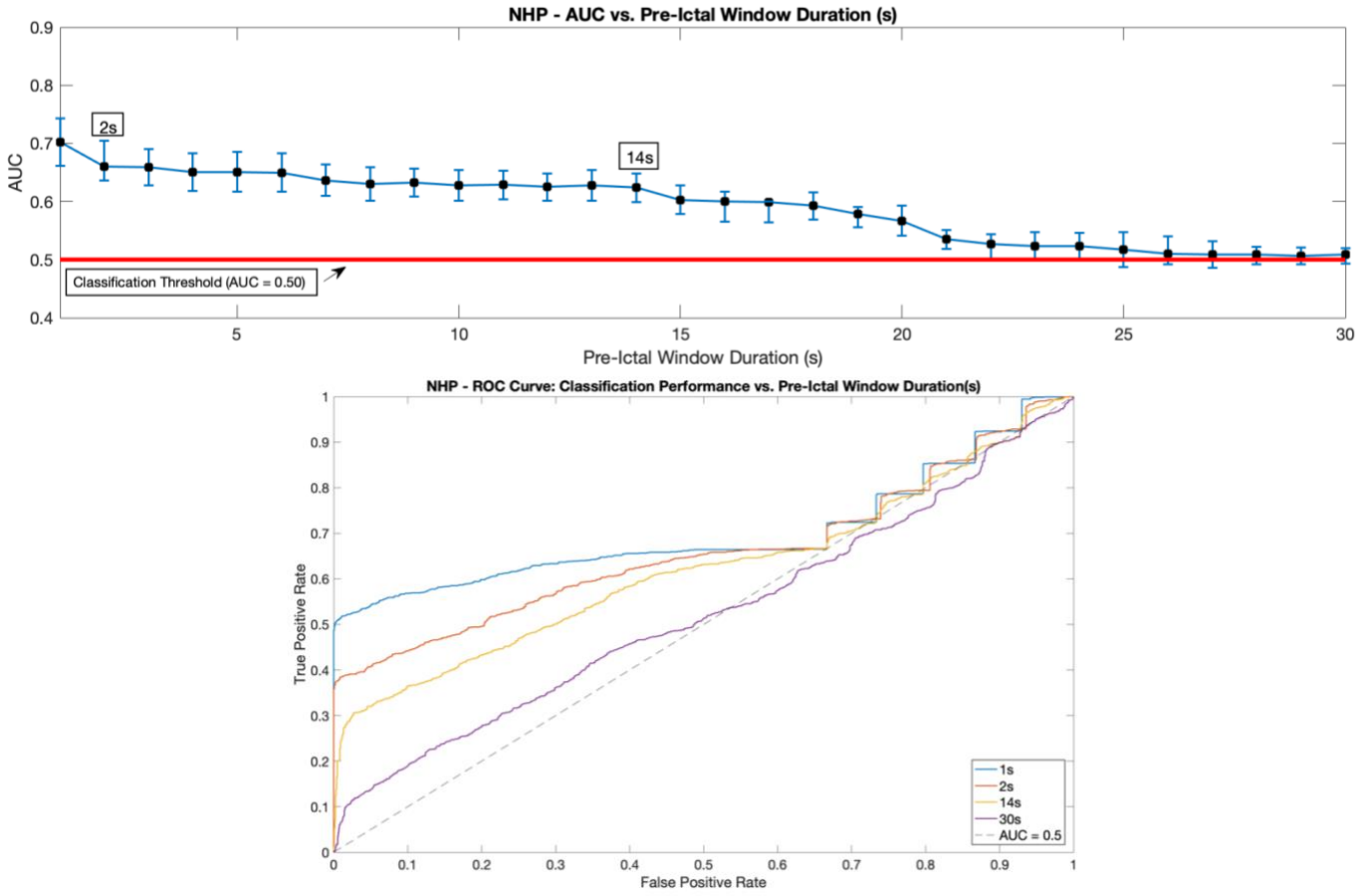

Fig. 4: *NHP analysis results. (Top) The corresponding AUC values for each pre-ictal window duration are plotted with confidence intervals for the AUC values depicted as vertical bars. (Bottom) ROC curves of key pre-ictal window durations plotted. The first and last ROC curves correspond to the longest and shortest window length and the third and fourth ROC curves correspond to the start and stop of an AUC plateau.*

For the single NHP, ROC curves for each window length corresponding to a hypothesized pre-ictal window duration were initially calculated to determine classifier performance. Using these ROC curves, the AUC was calculated for each of the hypothesized pre-ictal window durations for the NHP-PCN model of epilepsy in order to determine the degree of separability between interictal and pre-ictal data for the respective window duration. The classification threshold is 0.5. If an AUC is at or below 0.5, we can assume that classification is primarily due

to chance (AUC = 0.5) or false positive rate is universally greater than true positive rate (AUC < 0.5).

Until a window duration of 26 seconds the AUC remains above 0.5; however, when we take into account confidence intervals, 21 seconds is the final window duration that has an AUC above 0.5. More notably, however, we can identify an AUC plateau around an AUC of 0.65 for window durations of 2 seconds to 14 seconds, with lower bound confidence intervals never crossing an AUC of 0.6 (Fig. 4). In addition, the ROC curves of the bounds of this plateau (2s, 14s) are very similar, which indicates that both window durations contain distinguishable pre-ictal window data (Fig. 4). Preceding this AUC plateau is the peak AUC of 0.70 at a pre-ictal window duration of 1 second. Proceeding the AUC plateau is a steady decline in AUC beginning with a pre-ictal window duration of 15 seconds. Beyond this continuous decline in AUC following the AUC plateau period (2s – 14s), no sharp dip in AUC was visualized after any other window duration.

B. Rat-TeNT – Individual Rat Analysis

For the analysis of Rat-TeNT data, results are broken up into N = 3 individual rats' results and then a joint analysis of all rats' (N = 11) seizure recordings (n = 200).

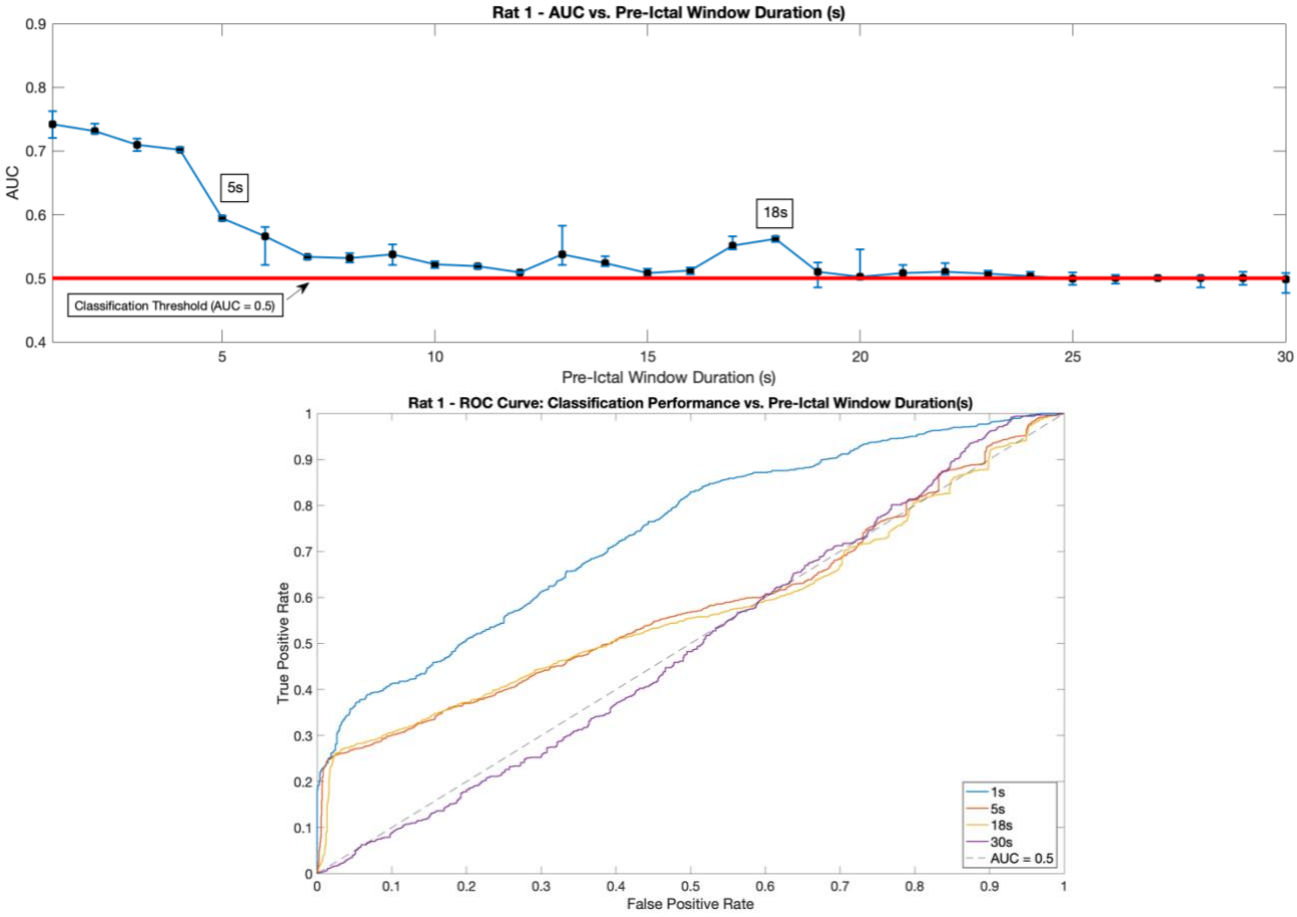

Fig. 5: *Rat 1 analysis results. (Top) The corresponding AUC values for each pre-ictal window duration are plotted with confidence intervals for the AUC values depicted as vertical bars. (Bottom) ROC curves of key pre-ictal window durations plotted. The first and last ROC curves correspond to the longest and shortest window length and the third and fourth ROC curves correspond to the start and stop of an AUC plateau.*

For Rat 1, ROC curves for each window length corresponding to a hypothesized pre-ictal window duration were initially calculated to determine classifier performance. Using these ROC curves, the AUC was calculated for each of the hypothesized pre-ictal window durations for Rat 1 of the Rat-TeNT model of epilepsy in order to determine the degree of separability between interictal and pre-ictal data for the respective window duration. The classification threshold is

0.5. If an AUC is at or below 0.5, we can assume that classification is primarily due to chance (AUC = 0.5) or false positive rate is universally greater than true positive rate (AUC < 0.5).

Until a window duration of 18 seconds the AUC remains above 0.5 with confidence intervals taken into account. We can identify an AUC plateau around an AUC of 0.51-0.52 for window durations of 7 seconds to 17 seconds, with lower bound confidence intervals never crossing an AUC of 0.5 (Fig. 5). In addition to this plateau, window durations from 5 seconds to 18 seconds show a steady pattern in AUC holding above 0.5 and staying under 0.6. Also, of note, the ROC curves of the bounds of this plateau (5s, 18s) are practically identical, which indicates that both windows contain distinguishable pre-ictal data (Fig. 5). Pre-ictal window durations less than 5 seconds have AUC's greater than 0.7. Beyond a window duration of 18 seconds, the AUC of all subsequent windows is either at or below 0.5 or has a lower bound confidence interval at or below 0.5.

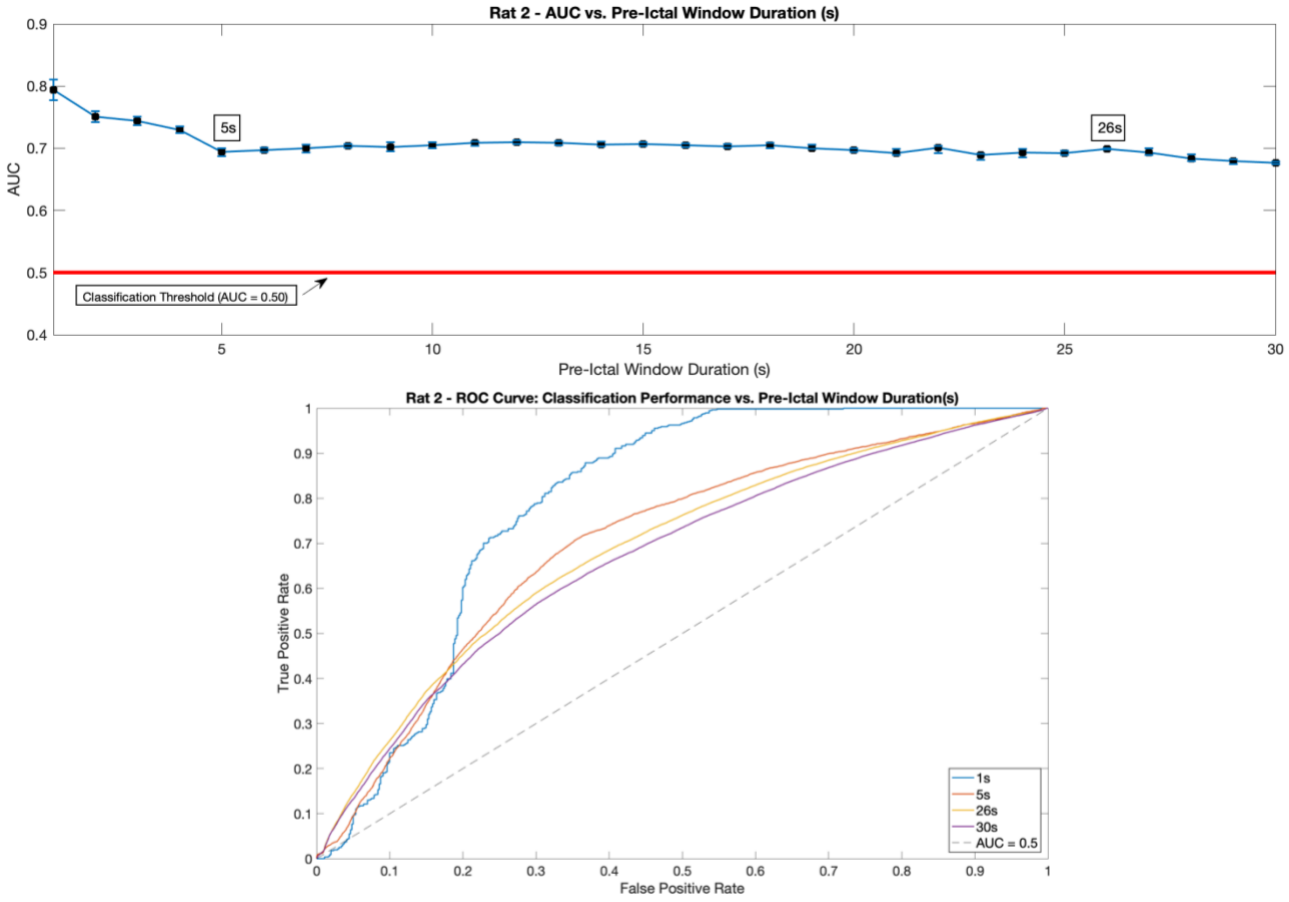

Fig. 6: *Rat 2 analysis results. (Top) The corresponding AUC values for each pre-ictal window duration are plotted with confidence intervals for the AUC values depicted as vertical bars. (Bottom) ROC curves of key pre-ictal window durations plotted. The first and last ROC curves correspond to the longest and shortest window length and the third and fourth ROC curves correspond to the start and stop of an AUC plateau.*

For Rat 2, ROC curves for each window length corresponding to a hypothesized pre-ictal window duration were initially calculated to determine classifier performance. Using these ROC curves, the AUC was calculated for each of the hypothesized pre-ictal window durations for Rat 2 of the Rat-TeNT model of epilepsy in order to determine the degree of separability between interictal and pre-ictal data for the respective window duration. The classification threshold is 0.5. If an AUC is at or below 0.5, we can assume that classification is primarily due to chance (AUC = 0.5) or false positive rate is universally greater than true positive rate (AUC < 0.5).

The AUC remains above 0.5 with confidence intervals taken into account at all window durations (1s-30s) (Fig. 6). We can identify an AUC plateau around an AUC of 0.70 for window durations of 5 seconds to 26 seconds, with lower bound confidence intervals never crossing an AUC of 0.5 (Fig. 6). Window durations from 1 seconds to 4 seconds show relatively high AUC's as they are above 0.75, with small confidence intervals. Even after the plateau of 26 seconds, although AUC begins to decline, it stays above 0.50 at all subsequent pre-ictal window durations from 27 seconds to 30 seconds. The ROC curve for 5 seconds looks very similar to the ROC curve for 25 seconds, which indicates that both windows contain distinguishable pre-ictal data (Fig. 6). However, the ROC curve for 30 seconds also looks similar to those of smaller pre-ictal window durations. This may suggest that the pre-ictal window may extend beyond 30 seconds pre-seizure. This may also suggest that the logistic regression model may have overfit this data by memorizing it, which may be due to the fact that Rat 2 had the fewest seizures (n = 20) to train and test on compared to Rat 1 (n = 49) and Rat 3 (n = 54).

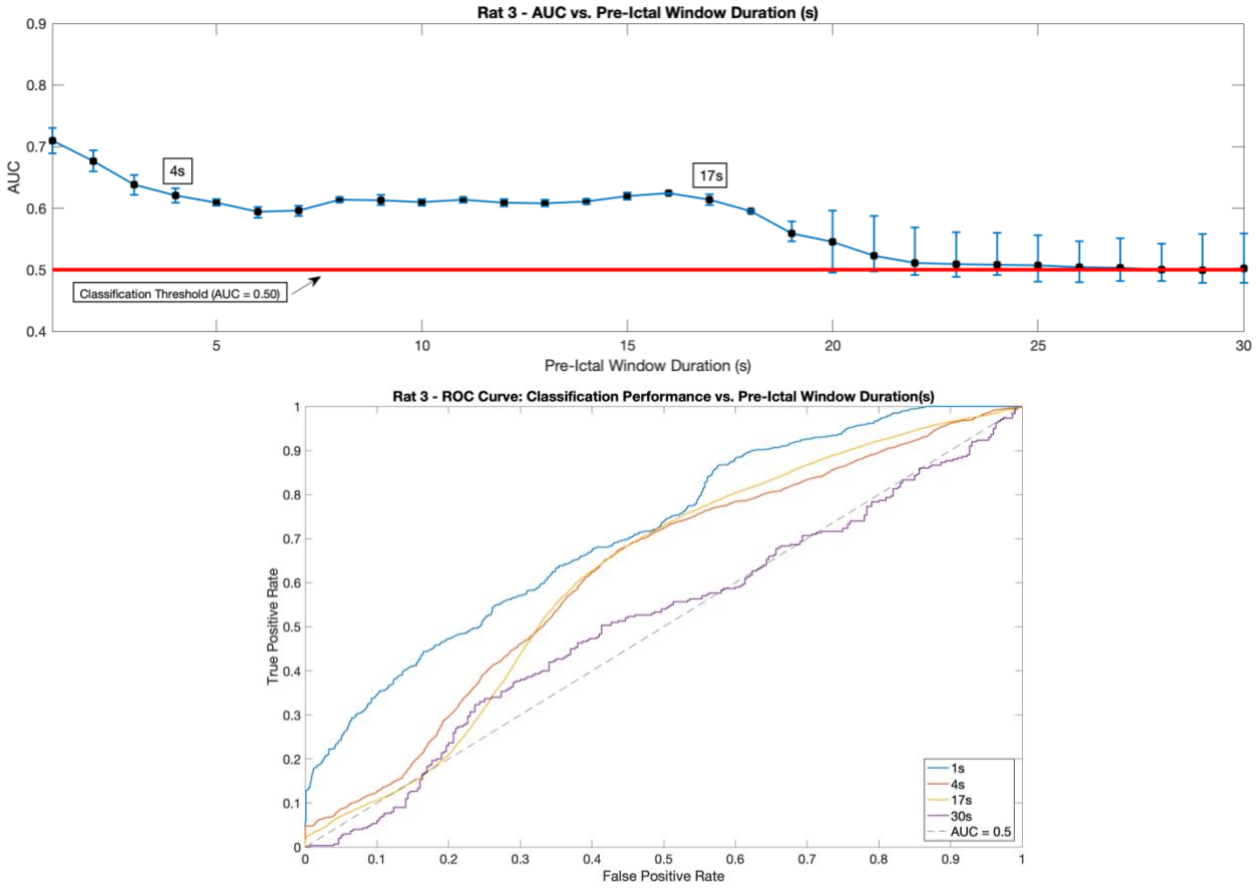

Fig. 7: *Rat 3 analysis results. (Top) The corresponding AUC values for each pre-ictal window duration are plotted with confidence intervals for the AUC values depicted as vertical bars. (Bottom) ROC curves of key pre-ictal window durations plotted. The first and last ROC curves correspond to the longest and shortest window length and the third and fourth ROC curves correspond to the start and stop of an AUC plateau.*

For Rat 3, ROC curves for each window length corresponding to a hypothesized pre-ictal window duration were initially calculated to determine classifier performance. Using these ROC curves, the AUC was calculated for each of the hypothesized pre-ictal window durations for Rat 3 of the Rat-TeNT model of epilepsy in order to determine the degree of separability between interictal and pre-ictal data for the respective window duration. The classification threshold is 0.5. If an AUC is at or below 0.5, we can assume that classification is primarily due to chance (AUC = 0.5) or false positive rate is universally greater than true positive rate (AUC < 0.5).

Until a window duration of 20 seconds the AUC remains above 0.5 with confidence intervals taken into account. We can identify an AUC plateau around an AUC of 0.63-0.64 for window durations of 4 seconds to 17 seconds, with lower bound confidence intervals never crossing an AUC of 0.5 (Fig. 7). In addition to this plateau, window durations from 4 seconds to 17 seconds show a steady pattern in AUC holding above 0.6 and staying under 0.7. Of note, the ROC curves of the bounds of this plateau (4s, 17s) are practically identical, which indicates that both windows contain distinguishable pre-ictal data (Fig. 7). Pre-ictal window durations less than 4 seconds having decreasing AUC from 1 second window to the 3 second window, before stabilization at 4 seconds. Beyond a window duration of 17 seconds, the AUC of all subsequent windows, except for a pre-ictal window 18s and 19s, is either at or below 0.5 or has a lower bound confidence interval at or below 0.5.

It is worth noting that the confidence intervals are much larger in window durations equal or greater than 20 second when compared to shorter window durations less than 20 seconds. This increased variability associated with a lower AUC overall may be due to interictal spikes being included in the interictal window data. This may resemble the pre-ictal window and, thus, reduce overall AUC due to a poorer ability to discriminate even though the window may still contain a good amount of pre-ictal data. The increased variability may also simply be due to artifact.

C. Rat-TeNT – Joint Rat Analysis

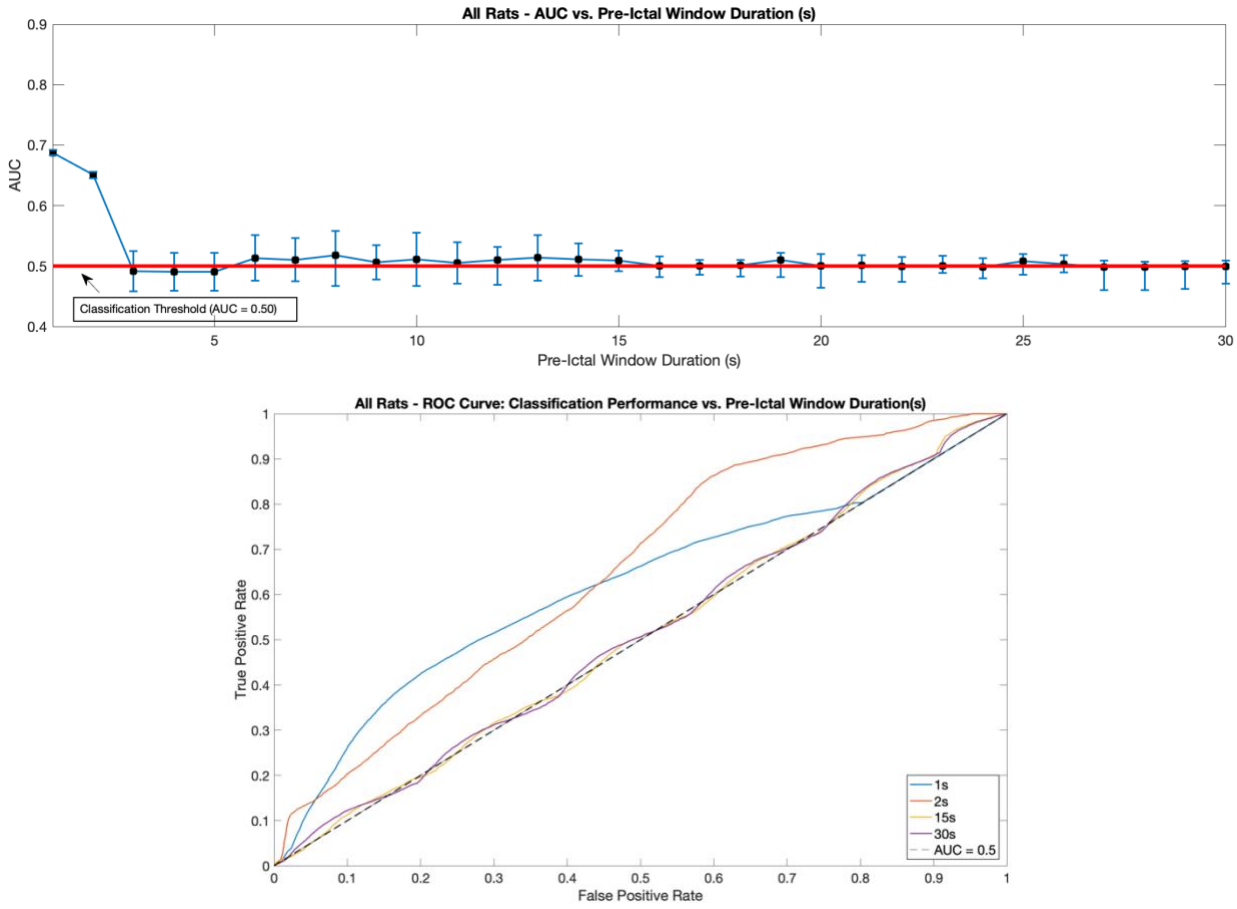

Fig. 8: *Joint rat analysis results. (Top) The corresponding AUC values for each pre-ictal window duration are plotted with confidence intervals for the AUC values depicted as vertical bars. (Bottom) ROC curves of key pre-ictal window durations plotted. The first and last ROC curves correspond to the longest and shortest window length and the third and fourth ROC curves correspond to the start and stop of an AUC plateau. Note: No distinct plateau showing successful classification observed.*

For all rats (N = 11), ROC curves for each window length corresponding to a hypothesized pre-ictal window duration were initially calculated to determine classifier performance. Using these ROC curves, the AUC was calculated for each of the hypothesized pre-ictal window durations for the joint analysis Rat-TeNT model of epilepsy in order to determine the degree of separability between interictal and pre-ictal data for the respective window duration. The classification threshold is 0.5. If an AUC is at or below 0.5, we can assume that classification is

primarily due to chance (AUC = 0.5) or false positive rate is universally greater than true positive rate (AUC < 0.5).

Pre-ictal window durations of greater than 2 seconds caused the AUC to remain at or below 0.5 with confidence intervals taken into account (Fig. 8). This means that our pre-ictal window classifier identified a brief 2 second common pre-ictal duration across all rats. AUC only remains above 0.5 for window duration of 1 and 2 seconds. There is a sharp decline in AUC from 0.68 at window duration of 2 seconds to below 0.5 at window duration of 3 seconds. After a window duration of 3 seconds, the AUC scores do not surpass 0.5, with confidence intervals taken into account. The ROC curves show that classification occurs by chance, as there is an equal rate of false positives as there are true positives for pre-ictal window durations greater than 2 seconds.

IV. Discussion

By using a sliding window, we were able to test a spectrum of ground truths for a hypothesized pre-ictal window duration. The results of our study reveal that a pre-ictal window characterizing the transition from the intertidal state to the ictal state can be distinguished within the baseline interictal window. Although our results do not allow us to confidently identify a singular, clear-cut pre-ictal duration, we showed that our classifier was able to distinguish between the pre-ictal and interictal window for a variety of window durations. Discrimination was apparent when the AUC was greater than 0.5 or there was an AUC plateau, which consisted of several window durations presenting with similar AUC results and similar ROC curves. These findings indicate that our classifier was able to discriminate between the two windows (interictal and pre-ictal) as it detected underlying differences in the features that it was trained and tested on for each respective window. Our results showed variability when it came to the model of epilepsy we were training and testing on and whether we were attempting to classify pre-ictal windows on an individual animal's seizures or seizures jointly across all animals of a respective model. In this case, only the Rat-TeNT model had multiple animals.

Since there was only data available from one NHP, we were unable to see if our algorithm could generalize across multiple NHPs with PCN-induced seizures. However, from analysis of the single NHP, we were able to identify an AUC Plateau from a pre-ictal window duration of 2 seconds to a pre-ictal window duration of 14 seconds. After this 14 second window, AUC steadily declined until it eventually reached 0.5. This plateau period was also characterized by similar ROC curves. Altogether this means that within each of the windows, there existed some pre-ictal characteristics that differentiated them from interictal windows. Although we know what ENFs were used for classification purposes, we have yet to study how these features are implicated in

the transition from non-seizure to seizure. Since our model allows us to pinpoint objectively determined, pre-ictal window lengths of interest, it will allow for further investigation into the exact behavior of these features, such as theta power, in the time segment we have identified as prone to seizure. Having a better understanding of key seizure-onset biomarkers will not only expand our current understanding seizure dynamics, but also may increase the potential for the development of better prophylactic neural modulation treatments (i.e. proactive, rather than reactive).

It is also important to note that our classifier appeared to be able to generalize across multiple days of recordings for the NHP, as we were able to discern a pre-ictal window duration; however, more data and a new cross validation approach will be necessary to give more credibility to our classifier's generalization ability. Our train and test sets consisted of randomized interictal windows. This means that our classifier might have had a train set that had a sample of interictal windows from all of the recording sessions, which means the classifier may have overfit to our NHP-PCN data. Since PCN-induced seizures appear to be heterogenous between different recording sessions, it is possible that precise mechanism of transition from baseline to seizure may have varied between sessions. Therefore, a stronger test of generalizability would be to have a train test consisting of interictal windows from the same day of recording and then tested on interictal windows from different days of recordings. However, due to the limited quantity of data we had for each recording session, this cross-validation approach was unable to be performed. Therefore, in order to further validate whether or not our classifier can truly generalize between multiple days of seizure presentation and different cross-validation approach, along with more data per recording session will be necessary. Another approach would be to compare multiple NHPs and see if our classifier could generalize across animals. In order to test this possibility, we

conducted a joint analysis of all TeNT rats; however, it is important to note that in order to keep results consistent, the rat-TeNT data was cross-validated in the same manner as the NHP-PCN data.

Classification of the pre-ictal window using our sliding window method on individual rats revealed potential evidence for several unique pre-ictal window lengths for each animal. Each animal's pre-ictal window classification varied, as the pre-ictal window duration that preceded the AUC falling to or below 0.5 was different for all 5 animals. However, as seen in the NHP, a general trend that emerged was the presence of an AUC plateau after an initial drop-off in AUC, which was typically in the earlier windows, and a second drop-off in AUC, which would be followed by a steady decline until an AUC of 0.5 was reached. The shorter pre-ictal windows, usually 1-3 seconds, had much higher AUCs than that of pre-ictal window durations within the AUC plateaus. This first drop-off in AUC may occur due to the detection of a propagating seizure from adjacent neural tissue. A limitation of our recording methods is that we cannot be 100% certain that the seizure onset we see on EEG is the true seizure onset time. We may be detecting a seizure that has already started in adjacent neural tissues. This limitation would create outlier data in the shorter pre-ictal windows as they are closer to seizure onset and now may actually contain some seizure data. This will inevitably lead to a higher AUC due to how distinct seizure data and interictal data is.

The second drop-off in AUC is more in-line with what we expected. This second drop-off, which is followed by a steady decline in AUC until 0.5 is reached, could be signaling the transition point between the interictal window and pre-ictal window. Since there is an "AUC plateau" present before the second drop-off in AUC, it is reasonable to think that this plateau may be our best estimate of the pre-ictal window's duration. Based on this logic, the start of Rat 1's pre-ictal

window may be 18 seconds prior to seizure onset, the start of Rat 2's pre-ictal window may be 26 seconds prior to seizure onset, and the start of Rat 3's pre-ictal window may be 17 seconds prior to seizure onset, as the second AUC drop-off and steady decline follows these pre-ictal window durations and indicates the end of the AUC plateau. Comparison of ROC curves amongst all the window durations within the AUC plateau reveals very similar curves, which implies that within each window, there exists some pre-ictal characteristics that differentiated them from interictal windows. This is similar to what we saw in the NHP.

Analysis of individual rats also revealed to us that the true pre-ictal window may not be the same for all individuals. Despite seizures being induced by the same models and the same conditions applied during surgery and recording sessions, all rats seemed to have a different estimated pre-ictal window duration at the end of their "AUC plateau". This may be due to the fact that the rodent TeNT model of epilepsy creates very heterogenous seizures. Therefore, each rat's presentation of "epilepsy" was most likely different. Although, this mirrors reality, as clinically, seizures may present differently across patients, as well.

In the joint analysis of all rats, our classifier was unable to provide us with any estimate of pre-ictal window duration with an associated AUC of above 0.5, except for window durations of 1 second and 2 seconds. Therefore, our classifier appeared to find a shortest common denominator of 2 seconds as a pre-ictal window across all rats. This may be evidence that the TeNT-induced seizure model consists of subject-specific pre-ictal window lengths. This finding makes sense as TeNT-induced seizures are very heterogenous in presentation in rodents. Furthermore, since each rat had appeared to have its own pre-ictal window duration, each animal may have its own unique mechanisms of transition to seizure. Therefore, our algorithm may have been unable to detect sufficient commonalties between transitions to seizure across all rats beyond the identified 2-

second pre-ictal window duration. Regardless, a 2-second pre-ictal window may still provide more clinical utility than a detection-based approach (RNS), as it increases the time-window to potentially abort an oncoming seizure if this window were to be used in a prediction-based neural modulation therapy.

Our tool has made it possible to quantitatively delineate the pre-ictal window on a subject-specific basis and compare the pre-ictal neural dynamics between different seizure models using a supervised machine learning model. This study provides the opportunity to gain valuable insight into the transition to seizure as we have identified potential estimates of the pre-ictal windows of individual rats, a common brief pre-ictal window in all rats, and the pre-ictal window of an individual NHP. A more in-depth analysis of these windows may reveal important information, such as the behavior of key ENFs or the identification of novel ENFs that characterize the pre-ictal window. More specifically, ENFs that characterize the pre-ictal window can be studied to better understand the transition from non-seizure to seizure and may be used to identify appropriate, subject-specific stimulation patterns for modulating neural state. With more data, better classification can be done using feature-learning algorithms, so as to continue improving our understanding of and ability to accurately identify the pre-ictal window.

Clinically, the identification of an accurate pre-ictal window may lead to more effective neural modulation therapies by developing a proactive approach, rather than a reactive approach. A direct application could be the deployment of a subject-specific pre-ictal classifier on future clinical devices. Future work would focus on developing a better classifier using more features and a more robust cross-validation approach, improving our understanding of the fluctuations of key ENFs during the pre-ictal window in order to better characterize the neural dynamics that underlie the transition to seizure, improving seizure prediction capabilities for use in neural

modulation therapeutics by curbing the practice of arbitrarily selected pre-ictal windows, and developing better subject-specific stimulation patterns for modulating neural state.

V. FIGURES

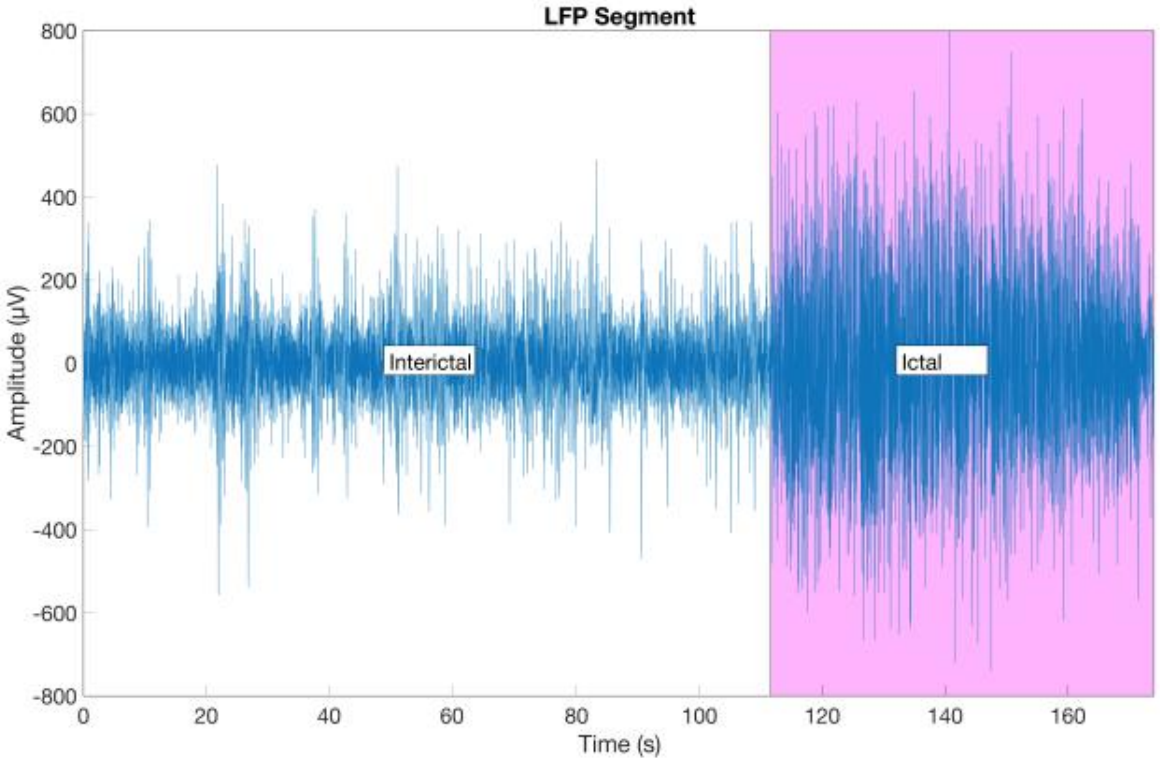

Fig. 1: *Annotated and segmented LFP from NHP-PCN used for subsequent feature extraction showing distinction between interictal and ictal periods.*

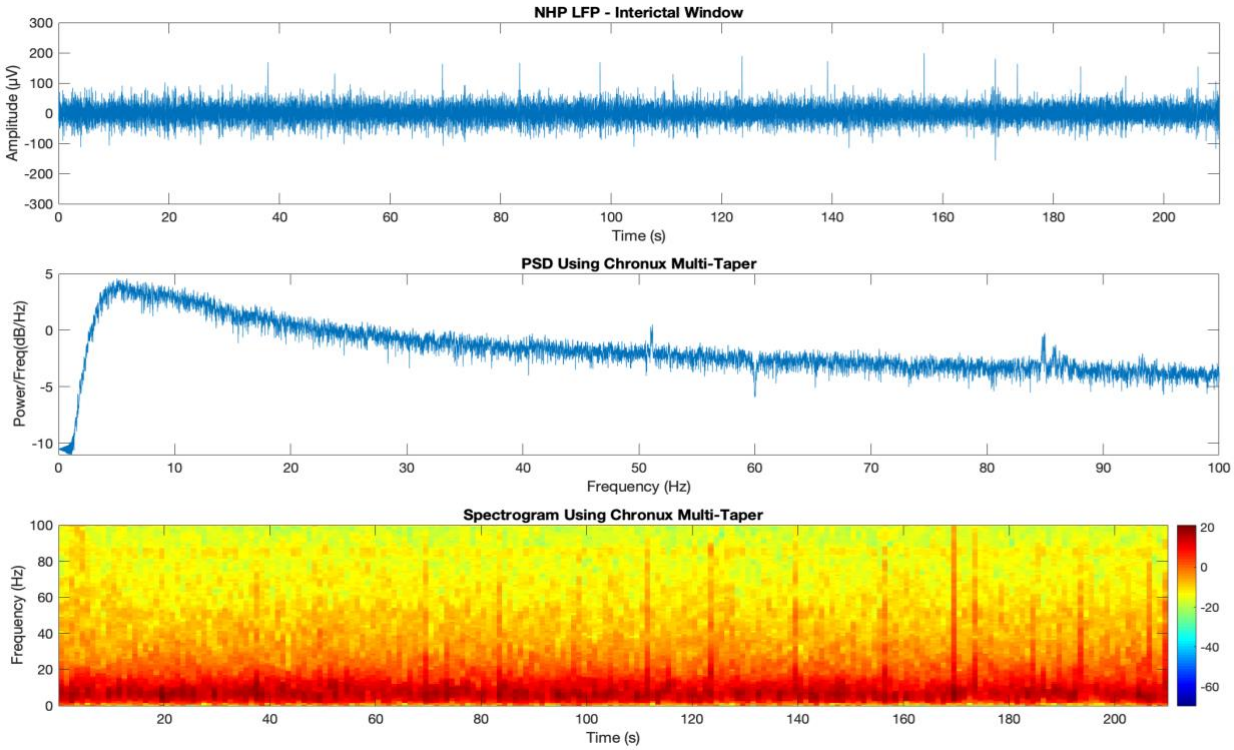

Fig. 2a: *Example of NHP-PCN interictal window presented in time domain, as a power spectral density, and as a spectrogram calculated using MTM. Depicts conversion from time to frequency domain in order to extract spectral features.*

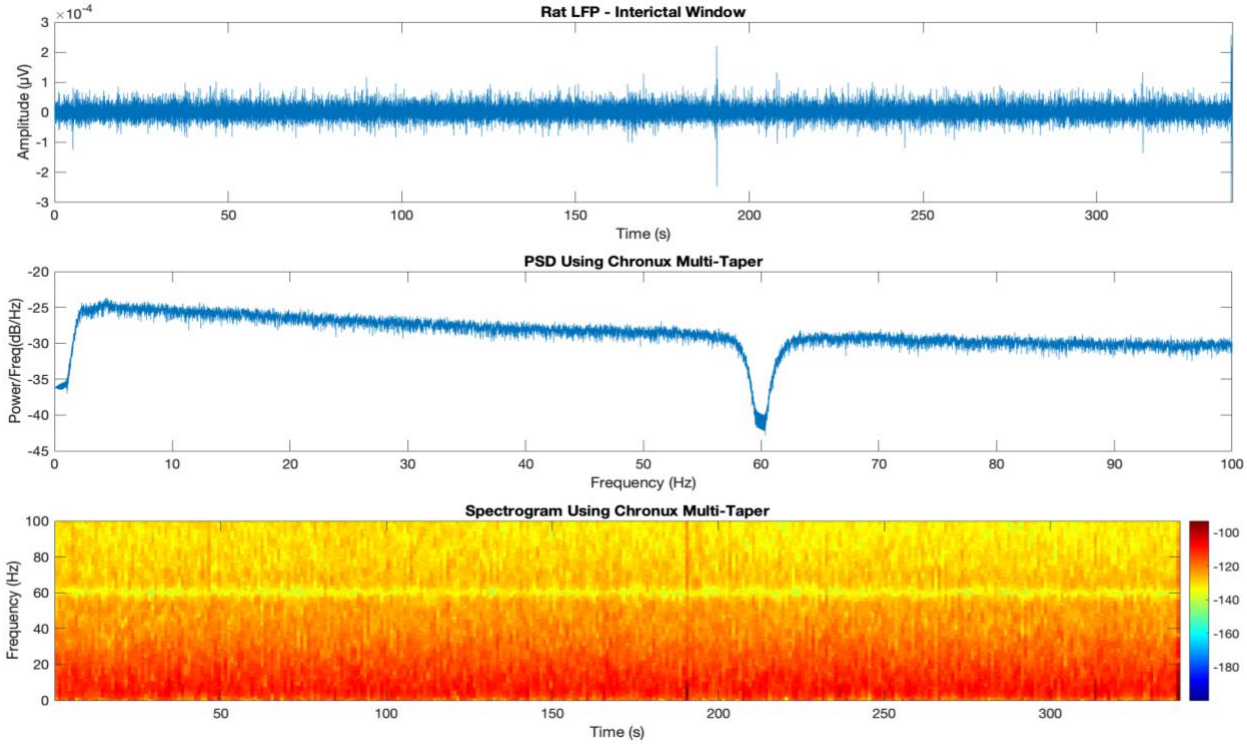

Fig. 2b: *Example of Rat-TeNT interictal window presented in time domain, as a power spectral density, and as a spectrogram calculated using MTM. Depicts conversion from time to frequency domain in order to extract spectral features.*

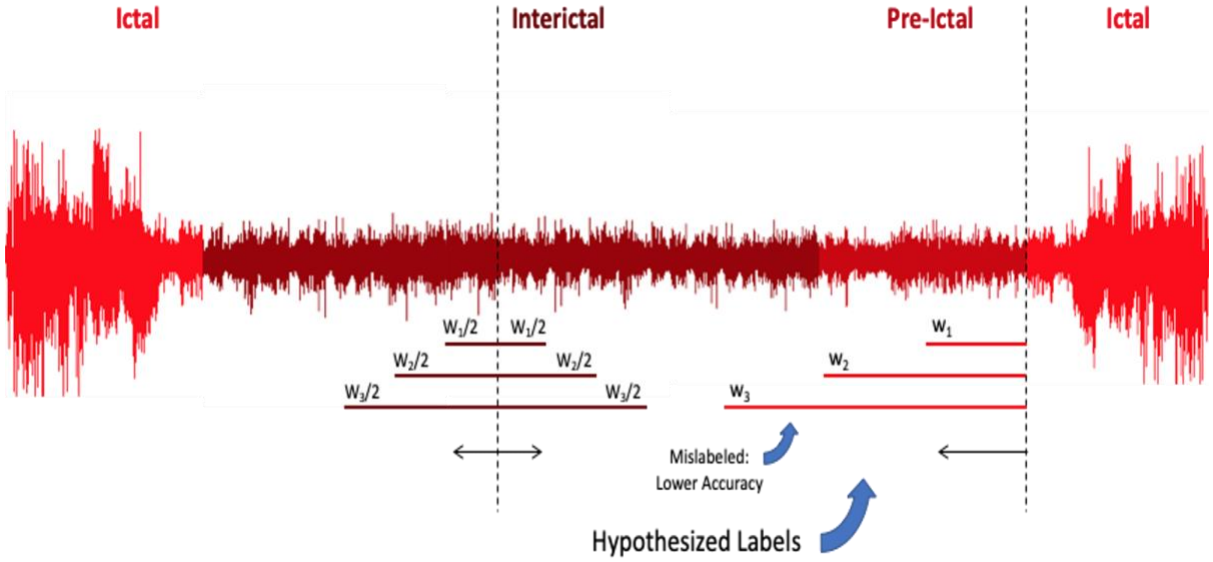

Fig. 3: *Diagram of logistic regression classifier with sliding window.*

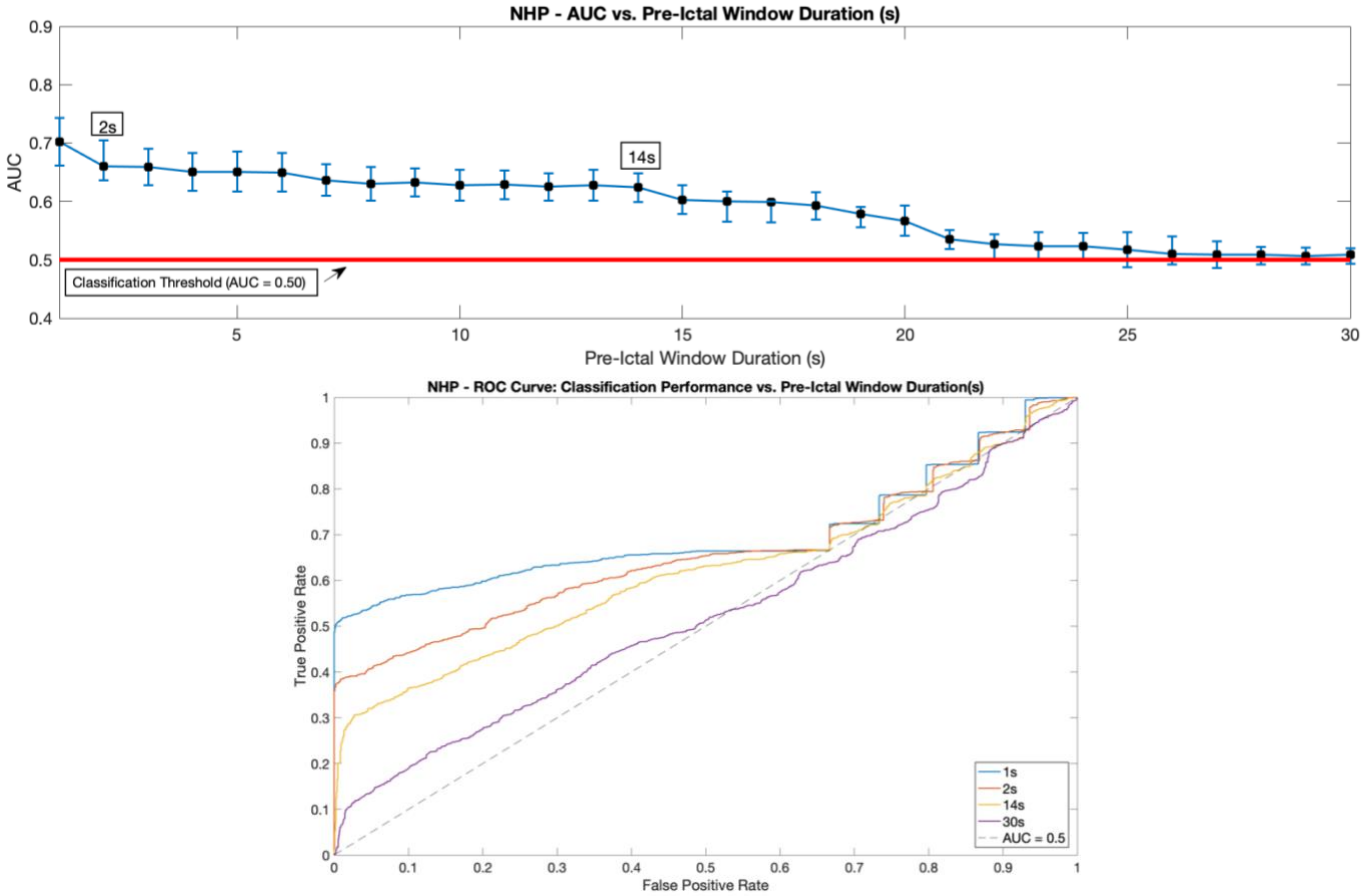

Fig. 4: *NHP analysis results. (Top) The corresponding AUC values for each pre-ictal window duration are plotted with confidence intervals for the AUC values depicted as vertical bars. (Bottom) ROC curves of key pre-ictal window durations plotted. The first and last ROC curves correspond to the longest and shortest window length and the third and fourth ROC curves correspond to the start and stop of an AUC plateau.*

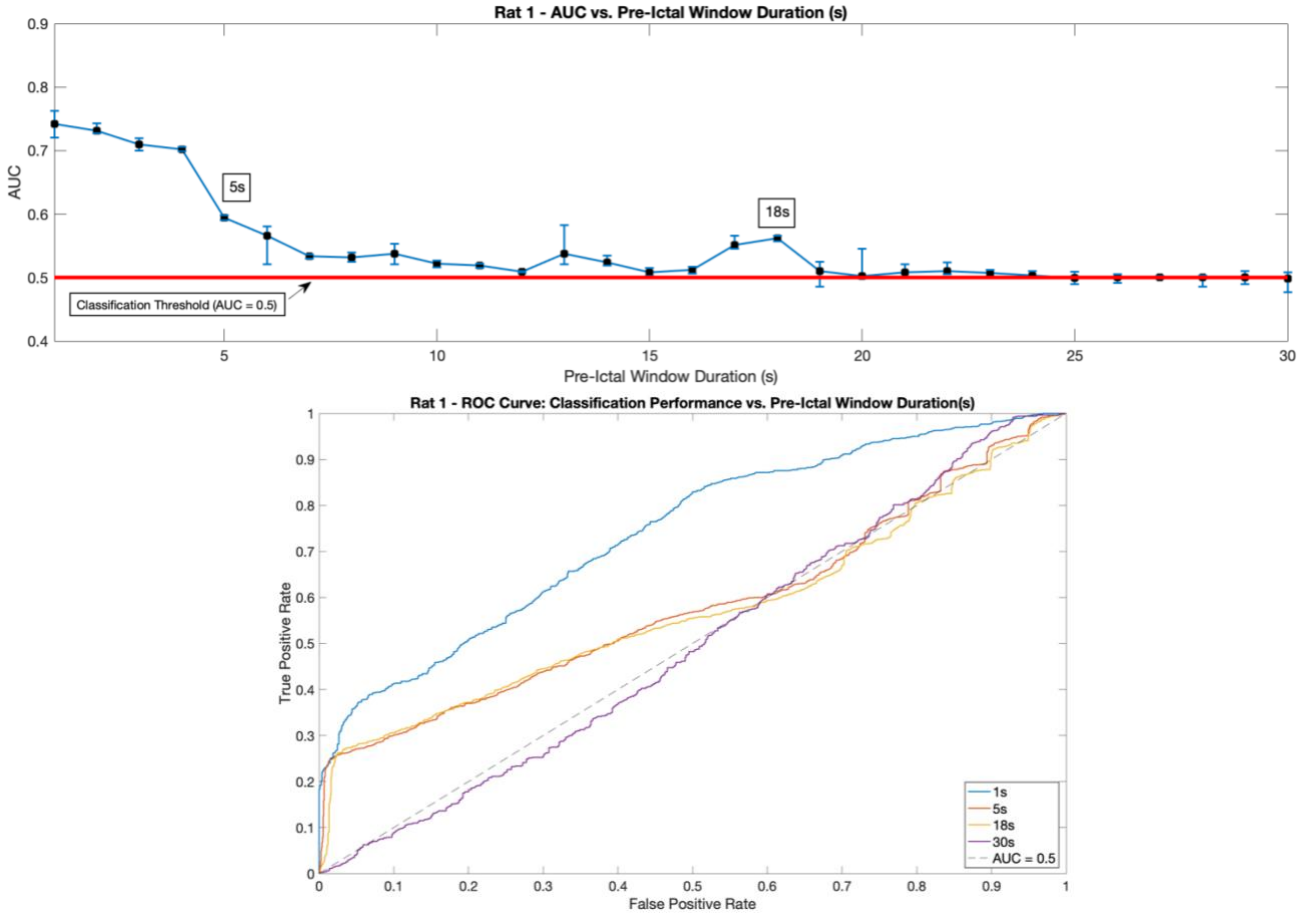

Fig. 5: *Rat 1 analysis results. (Top) The corresponding AUC values for each pre-ictal window duration are plotted with confidence intervals for the AUC values depicted as vertical bars. (Bottom) ROC curves of key pre-ictal window durations plotted. The first and last ROC curves correspond to the longest and shortest window length and the third and fourth ROC curves correspond to the start and stop of an AUC plateau.*

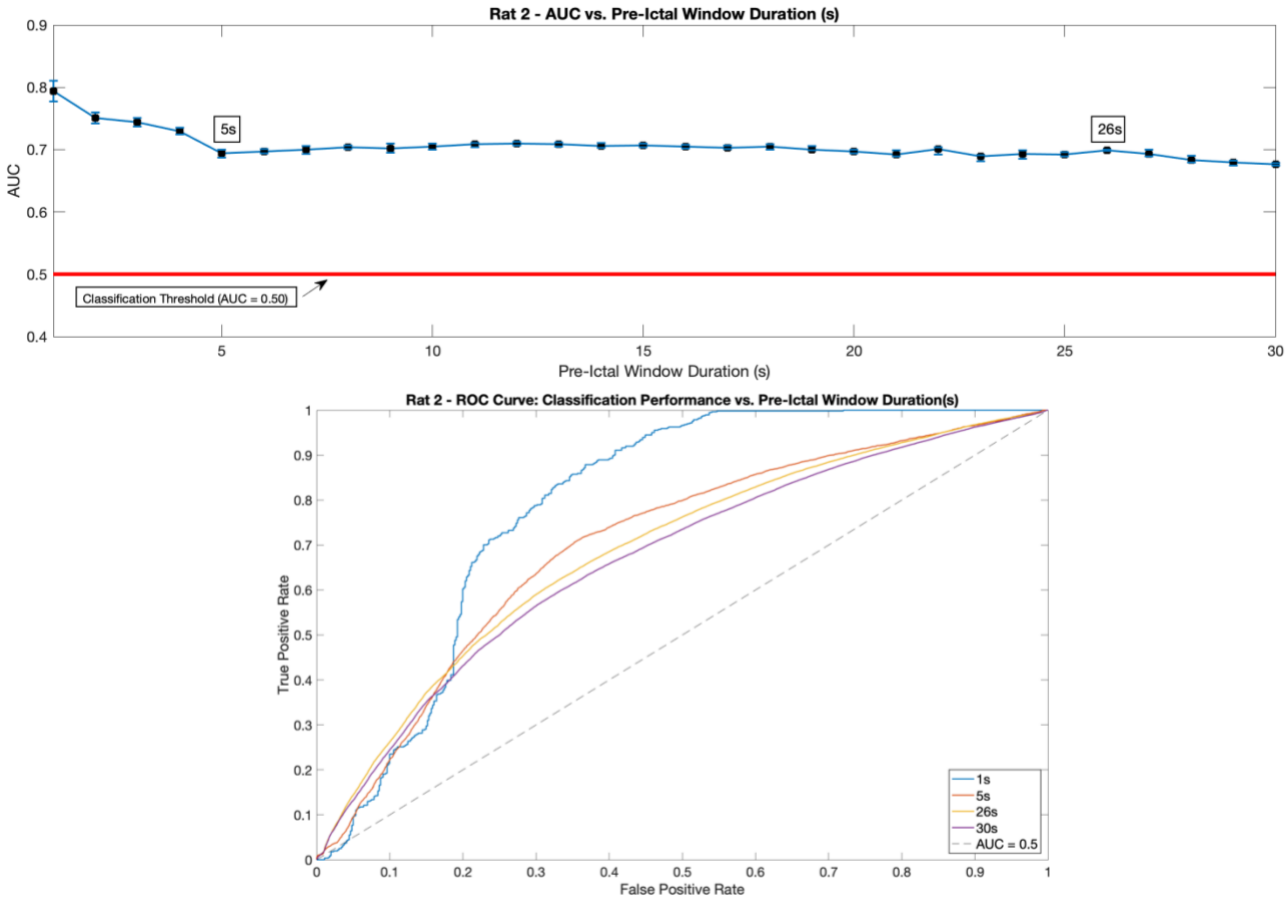

Fig. 6: *Rat 2 analysis results. (Top) The corresponding AUC values for each pre-ictal window duration are plotted with confidence intervals for the AUC values depicted as vertical bars. (Bottom) ROC curves of key pre-ictal window durations plotted. The first and last ROC curves correspond to the longest and shortest window length and the third and fourth ROC curves correspond to the start and stop of an AUC plateau.*

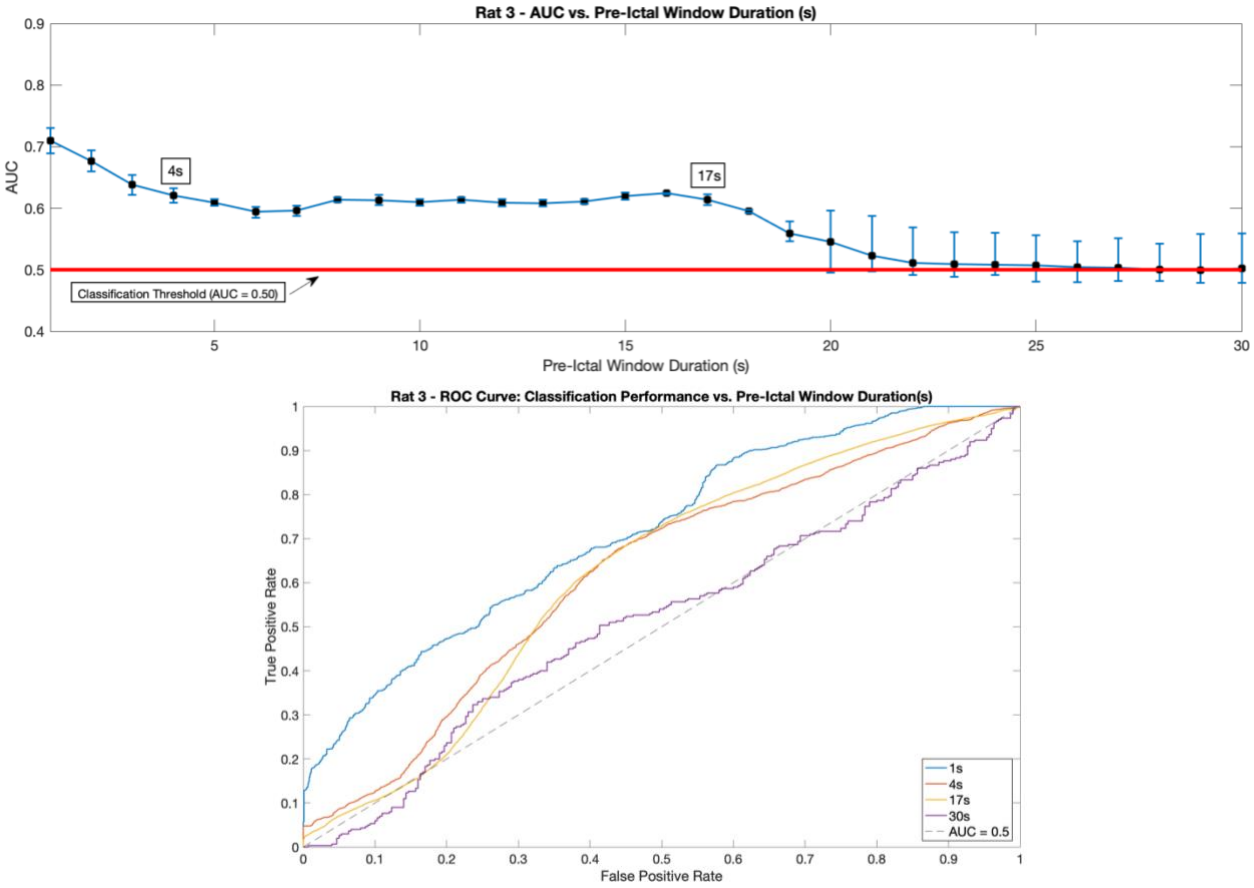

Fig. 7: *Rat 3 analysis results. (Top) The corresponding AUC values for each pre-ictal window duration are plotted with confidence intervals for the AUC values depicted as vertical bars. (Bottom) ROC curves of key pre-ictal window durations plotted. The first and last ROC curves correspond to the longest and shortest window length and the third and fourth ROC curves correspond to the start and stop of an AUC plateau.*

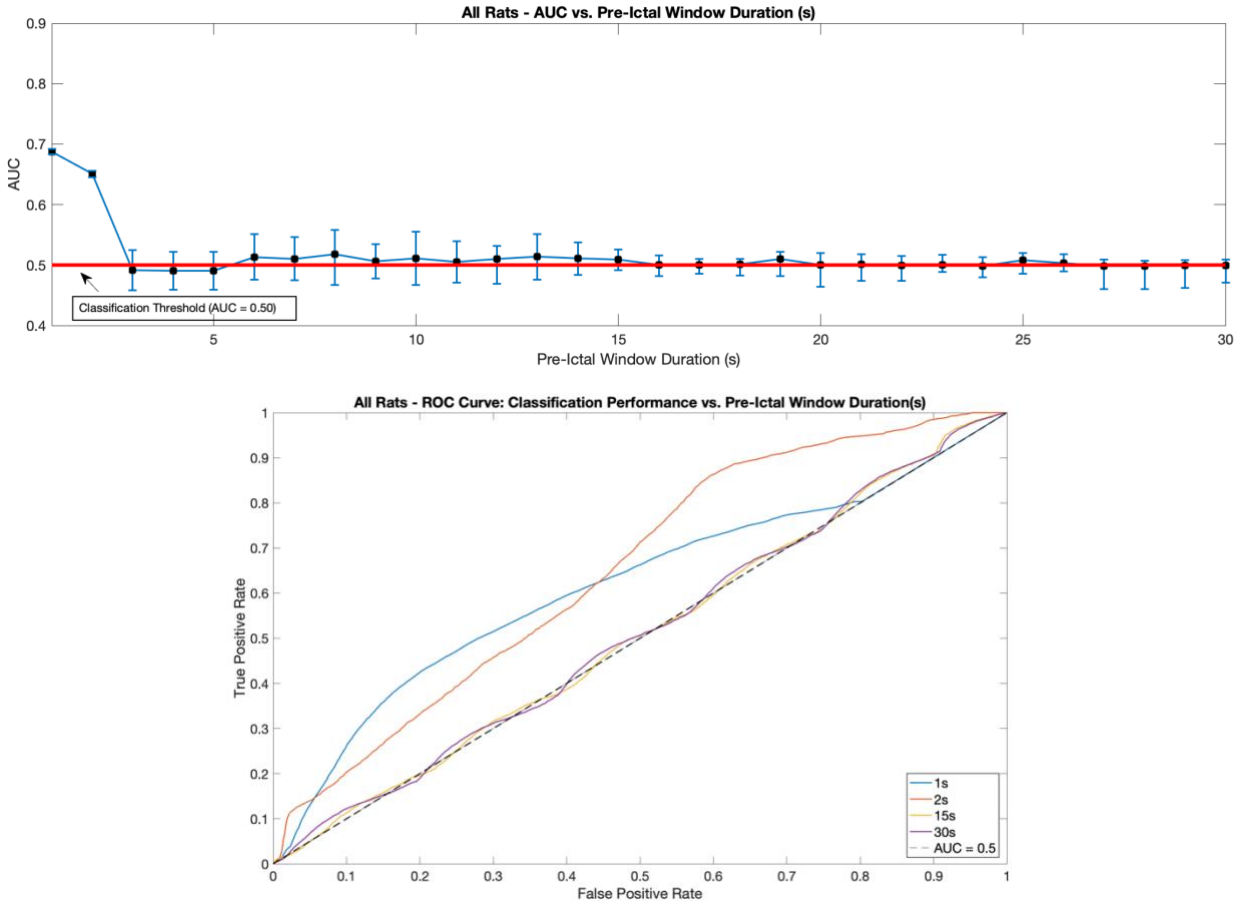

Fig. 8: *Joint rat analysis results. (Top) The corresponding AUC values for each pre-ictal window duration are plotted with confidence intervals for the AUC values depicted as vertical bars. (Bottom) ROC curves of key pre-ictal window durations plotted. The first and last ROC curves correspond to the longest and shortest window length and the third and fourth ROC curves correspond to the start and stop of an AUC plateau. Note: No distinct plateau showing successful classification observed.*

References

Al-Otaibi, F., Baeesa, S. S., Parrent, A. G., Girvin, J. P., & Steven, D. (2012). Surgical Techniques for the Treatment of Temporal Lobe Epilepsy. *Epilepsy Research and Treatment*, *2012*, 1–13. https://doi.org/10.1155/2012/374848

Alotaiby, T. N., Alshebeili, S. A., Alotaibi, F. M., & Alrshoud, S. R. (2017). Epileptic seizure prediction using CSP and LDA for scalp EEG signals. *Computational Intelligence and Neuroscience*, *2017*. https://doi.org/10.1155/2017/1240323

Babadi, B., & Brown, E. N. (2014). A review of multitaper spectral analysis. *IEEE Transactions on Biomedical Engineering*. IEEE Computer Society. https://doi.org/10.1109/TBME.2014.2311996

Barr, W. (2016). What happens to the brain following anterior temporal lobe resection? *Epilepsy Currents*, *16*(5), 316–318. https://doi.org/10.5698/1535-7511-16.5.316

Bewick, V., Cheek, L., & Ball, J. (2005, February). Statistics review 14: Logistic regression. *Critical Care*. https://doi.org/10.1186/cc3045

Blair, R. D. G. (2012). Temporal Lobe Epilepsy Semiology. *Epilepsy Research and Treatment*, *2012*, 1–10. https://doi.org/10.1155/2012/751510

Carney, P. R., Myers, S., & Geyer, J. D. (2011). Seizure prediction: Methods. *Epilepsy and Behavior*, *22*(SUPPL. 1). https://doi.org/10.1016/j.yebeh.2011.09.001

Cook MJ, O'Brien TJ, Berkovic SF, et al. Prediction of seizure likelihood with a long-term, implanted seizure advisory system in patients with drug-resistant epilepsy: a first-in-man study. *Lancet Neurol.* 2013;12(6):563–571. doi:10.1016/S1474-4422(13)70075-9

Desai, S. A., Rolston, J. D., McCracken, C. E., Potter, S. M., & Gross, R. E. (2016). Asynchronous Distributed Multielectrode Microstimulation Reduces Seizures in the Dorsal Tetanus Toxin Model of Temporal Lobe Epilepsy. *Brain Stimulation*, *9*(1), 86–100. https://doi.org/10.1016/j.brs.2015.08.008

Di Lorenzo, D. J., Leyde, K. W., & Kaplan, D. (2019). Neural state monitoring in the treatment of epilepsy: Seizure prediction—conceptualization to first-in-man study. *Brain Sciences*, *9*(7). https://doi.org/10.3390/brainsci9070156

England, M. J., Liverman, C. T., Schultz, A. M., & Strawbridge, L. M. (2012). *Epilepsy across the spectrum: Promoting health and understanding*. *Epilepsy Across the Spectrum: Promoting Health and Understanding* (pp. 1–537). National Academies Press. https://doi.org/10.17226/13379

Ghasemi, P., Sahraee, T., & Mohammadi, A. (2018). Closed- and Open-loop Deep Brain Stimulation: Methods, Challenges, Current and Future Aspects. *Journal of Biomedical Physics and Engineering*, *8*(2). https://doi.org/10.31661/jbpe.v8i2.898

Iasemidis, L. D. (2011, October). Seizure Prediction and its Applications. *Neurosurgery Clinics of North America*. https://doi.org/10.1016/j.nec.2011.07.004

Kiral-Kornek, I., Roy, S., Nurse, E., Mashford, B., Karoly, P., Carroll, T., … Harrer, S. (2018). Epileptic Seizure Prediction Using Big Data and Deep Learning: Toward a Mobile System. *EBioMedicine*, *27*, 103–111. https://doi.org/10.1016/j.ebiom.2017.11.032

Laxpati, N. G., Kasoff, W. S., & Gross, R. E. (2014). Deep Brain Stimulation for the Treatment of Epilepsy: Circuits, Targets, and Trials. *Neurotherapeutics*. Springer New York LLC. https://doi.org/10.1007/s13311-014-0279-9

Little, M. A., Varoquaux, G., Saeb, S., Lonini, L., Jayaraman, A., Mohr, D. C., & Kording, K. P. (2017, May 1). Using and understanding cross-validation strategies. Perspectives on Saeb et al. *GigaScience*. NLM (Medline). https://doi.org/10.1093/gigascience/gix020

Martin, R. C., Kretzmer, T., Palmer, C., Sawrie, S., Knowlton, R., Faught, E., … Kuzniecky, R. (2002). Risk to verbal memory following anterior temporal lobectomy in patients with severe left-sided hippocampal sclerosis. *Archives of Neurology*, *59*(12), 1895–1901. https://doi.org/10.1001/archneur.59.12.1895

Min, B., Guoming, L., & Jian, Z. (2013). Treatment of mesial temporal lobe epilepsy with amygdalohippocampal stimulation: A case series and review of the literature. *Experimental and Therapeutic Medicine*, *5*(4), 1264–1268. https://doi.org/10.3892/etm.2013.968

Myers, M. H., Jolly, E., Li, Y., de Jongh Curry, A., & Parfenova, H. (2017). Power spectral density analysis of electrocorticogram recordings during cerebral hypothermia in neonatal seizures. *Annals of Neurosciences*, *24*(1), 12–19. https://doi.org/10.1159/000464418

Nune, G., DeGiorgio, C., & Heck, C. (2015, October 28). Neuromodulation in the Treatment of Epilepsy. *Current Treatment Options in Neurology*. Current Science Inc. https://doi.org/10.1007/s11940-015-0375-0

Park, S. E., Laxpati, N. G., Gutekunst, C. A., Connolly, M. J., Tung, J., Berglund, K., … Gross, R. E. (2019). A Machine Learning Approach to Characterize the Modulation of the Hippocampal Rhythms Via Optogenetic Stimulation of the Medial Septum. *International Journal of Neural Systems*, *29*(10). https://doi.org/10.1142/S0129065719500205

Perucca, P., & Gilliam, F. G. (2012, September). Adverse effects of antiepileptic drugs. *The Lancet Neurology*. https://doi.org/10.1016/S1474-4422(12)70153-9

Sherdil, A., Chabardès, S., Guillemain, I., Michallat, S., Prabhu, S., Pernet-Gallay, K., … Piallat, B. (2018). An on demand macaque model of mesial temporal lobe seizures induced by unilateral intra hippocampal injection of penicillin. *Epilepsy Research*, *142*, 20–28. https://doi.org/10.1016/j.eplepsyres.2018.03.008

Stafstrom, C. E., & Carmant, L. (2015). Seizures and epilepsy: An overview for neuroscientists. *Cold Spring Harbor Perspectives in Biology*, *7*(5), 1–19. https://doi.org/10.1101/cshperspect.a022426

Schulze-Bonhage, A. (2017, January 1). Brain stimulation as a neuromodulatory epilepsy therapy. *Seizure*. W.B. Saunders Ltd. https://doi.org/10.1016/j.seizure.2016.10.026

Sun, F. T., & Morrell, M. J. (2014). Closed-loop Neurostimulation: The Clinical Experience. *Neurotherapeutics*. Springer New York LLC. https://doi.org/10.1007/s13311-014-0280-3

Willems, L. M., Watermann, N., Richter, S., Kay, L., Hermsen, A. M., Knake, S., … Strzelczyk, A. (2018). Incidence, risk factors and consequences of epilepsy-related injuries and accidents: A retrospective, single center study. *Frontiers in Neurology*, *9*(JUN). https://doi.org/10.3389/fneur.2018.00414

Zangiabadi, N., Ladino, L. Di., Sina, F., Orozco-Hernández, J. P., Carter, A., & Téllez-Zenteno, J. F. (2019). Deep brain stimulation and drug-resistant epilepsy: A review of the literature. *Frontiers in Neurology*. Frontiers Media S.A. https://doi.org/10.3389/fneur.2019.00601